



## Integrated Project

CLIMATE CHANGE AND IMPACT RESEARCH:  
THE MEDITERRANEAN ENVIRONMENT



### D 4.3.1 Data base of moisture balance for selected airsheds

Project No. 036961 – CIRCE

**Sixth Framework Programme**  
**6.3 Global Change and Ecosystems**

Start date of project: 01/04/07  
Due date of deliverable: 30/09/2008 (M18)

Duration: 48 months  
Actual Submission date: 13/01/09

Lead Partner for deliverable: CEAM  
Author: Petra Seibert, Irene Schicker, Sabine Radanovics

Project co-funded by the European Commission within the Sixth Framework Programme (2002-2006)		
Dissemination Level		
<b>PU</b>	Public	X
<b>PP</b>	Restricted to other programme participants (including the Commission Services)	
<b>RE</b>	Restricted to a group specified by the Consortium (including the Commission Services)	
<b>CO</b>	Confidential, only for members of the Consortium (including the Commission Services)	

---

## Document Release Sheet

<b><i>Distribution:</i></b>	All CIRCE consortium or Work Package members or Selected partners	<u>All CIRCE consortium</u>
-----------------------------	---	-----------------------------

---

## Table of Contents

<b>1. Publishable Executive Summary</b> .....	<b>5</b>
<b>2. Introduction</b> .....	<b>7</b>
<b>3. Data</b> .....	<b>8</b>
<b>4. Definition of Regions of Interest</b> .....	<b>10</b>
<b>5. Moisture and Precipitation Budgets</b> .....	<b>11</b>
5.1. Methods for the moisture budget evaluation.....	11
5.2. Mediterranean moisture budgets.....	13
5.3. Moisture budget of sub-basins.....	14
5.4. Methods for evaluation of precipitation budgets.....	14
5.5. Precipitation budgets of the Mediterranean as a whole.....	14
5.6. Precipitation budgets of sub-basins.....	14
<b>6. Residence Times, Recirculation and Stagnation</b> .....	<b>14</b>
6.1. Residence times.....	14
6.1.1. 1-day transport time.....	14
6.1.2. 5-day transport time.....	14
6.1.3. 30-day transport time.....	14
6.1.4. 90-day transport time.....	14
6.2. Stagnation and Recirculation.....	14
6.2.1. Stagnation.....	14
6.2.2. Recirculation.....	14
<b>7. Conclusions</b> .....	<b>14</b>
<b>8. References</b> .....	<b>14</b>

## List of Figures

Figure 1: Air streams to (black) and from the Mediterranean (gray). .....	6
Figure 2: Land-Sea mask for the Mediterranean in a 1° x 1° resolution as used in this study. ....	9
Figure 3: Definition of the sub-basins used. 1 Western Mediterranean, 2 Central Mediterranean, 3 Adriatic Sea, 4 Eastern Mediterranean, 5 Balearics, 6 Etesian, 7 Cyprus. ....	10
Figure 4: Mixing ratio of Mediterranean moisture and moisture outside the Mediterranean for the four seasons. ....	14
Figure 5: Fraction of moisture from Western Mediterranean basin for the four seasons. ....	14
Figure 6: Same as Fig. 5 but for the Central Mediterranean basin. ....	14
Figure 7: Same as Fig. 5 but for the Eastern Mediterranean basin. ....	14
Figure 8: Same as Fig. 5 but for the Balearics. ....	14
Figure 9: Same as Fig. 5 but for the Adriatic Sea. ....	14
Figure 10: Same as Fig. 5 but for the Etesian basin. ....	14
Figure 11: Same as Fig. 5 but for the Cyprus basin. ....	14
Figure 12: Mixing ratio of the precipitation originating in the Mediterranean to the total precipitation for the four seasons. ....	14
Figure 13: Mixing ratio of the precipitation originating in the Western Mediterranean basin and other precipitation origin shown for the four seasons. ....	14
Figure 14: Same as Fig. 13 but for the Central Mediterranean basin. ....	14
Figure 15: Same as Fig. 13 but for the Eastern Mediterranean basin. ....	14
Figure 16: Same as Fig. 13 but for the Balearics. ....	14
Figure 17: Same as Fig. 13 but for the Adriatic Sea. ....	14
Figure 18: Same as Fig. 13 but for the Etesian basin. ....	14
Figure 19: Same as Fig. 13 but for the Cyprus basin. ....	14
Figure 20: Residence times for 1-day transport in forward mode of the Mediterranean basin for the vertical layer 0 – 1000 agl (top) and the whole troposphere (bottom). ....	14
Figure 21: Residence times for 1-day transport in backward mode of the Mediterranean basin for the vertical layer 0 – 1000 agl (top) and the whole troposphere (bottom). ....	14
Figure 22: Residence times for 5-day transport in forward mode of the Mediterranean basin for the vertical layer 0 – 1000 agl (top) and the whole troposphere (bottom). ....	14
Figure 23: Residence times for 5-day transport in backward mode of the Mediterranean basin for the vertical layer 0 – 1000 agl (top) and the whole troposphere (bottom). ....	14
Figure 24: Same as Fig. 20 but for 30-day transport times. ....	14
Figure 25: Same as Fig. 21 but for 30-day transport times. ....	14
Figure 26: Same as Fig. 20 but for 90-day transport times. ....	14
Figure 27: Same as Fig. 21 but for 90-day transport times. ....	14
Figure 28: Stagnation in the Mediterranean region for 1-day intervals. ....	14
Figure 29: Stagnation in the Mediterranean region for 5-day interval. ....	14
Figure 30: Recirculation in the Mediterranean region during 1-day time interval. ....	14
Figure 31: Recirculation in the Mediterranean region during 3-day time interval. ....	14
Figure 32: Recirculation in the Mediterranean region during 5-day time interval. ....	14

---

## 1. Publishable Executive Summary

The aim of this deliverable D 4.3.1 was to create a data base of moisture and precipitation budgets for selected airsheds in the Mediterranean basin. Data of a global domain-filling simulation with the Lagrangian particle dispersion model FLEXPART, provided by Andreas Stohl (NILU), have been used. These data are available for the period October 1999 to April 2005. Residence times, stagnation and recirculation indices have also been evaluated with this data set.

The data base includes annual and seasonal means for different time intervals of:

- moisture evaluation
- precipitation evaluation
- residence times in forward and backward mode
- stagnation
- recirculation

and, where appropriate, a number of sub-basins of the Mediterranean region.

The fraction of atmospheric moisture over the Mediterranean region originating from the Mediterranean itself is highest in the summer season, between 50% and 70%. Moisture originating in the Mediterranean basin makes a contribution, although with a very low fraction, in the whole northern hemisphere. The Western Mediterranean influences mainly Europe, the Eastern parts Africa and the Middle East. On a smaller scale, for example moisture from the Adriatic Sea is relevant for the Balkan countries, Austria and the Po Basin in Northern Italy. Precipitation analyses gives results similar to that of the moisture analysis. The fraction of precipitation in the Mediterranean region which stems from the regions itself exceeds 40% in all seasons, with up to 70% regionally in summer. The higher SSTs in autumn increase the Mediterranean precipitation fraction. On a smaller scale, for example the Western Mediterranean is contributing relatively little precipitation on the Iberian peninsula, exceeding 20% only in spring and summer. However, the small region defined as the Balearic sub-basin seems to have a significant influence on the adjacent portion of Spain.

90-day residence times show very clearly that the Mediterranean is a crossroad of air streams: the air enters the Mediterranean mainly from the Northwest, while the outflow is split into two big flows with opposite direction through Central Asia to the Pacific coast, and over Northern Africa into the tropical Atlantic (Figure 1:). High-latitude regions over the North Atlantic and Canada are part of the source regions, but the outflow does not enter high latitudes within 90 days. Channelling by mountains and sea straits is visible especially in the 5-day and 30-d residence times. A channelled outflow route is over Mesopotamia, a low land between the high lands of Iran and Arabia, while the Gulf of Lyon between the Pyrenees and the Alps is a preferred inflow channel. In general, longer residence times are found over the Western and Central Mediterranean than over the Eastern

Mediterranean which is strongly influenced by the Etesian wind crossing the basin. Stagnation, defined as a short resultant wind vector over 1 day or 5 days, is strongly season-dependent. In winter and spring the Po Basin, the Adriatic Sea and the Region of Turkey-Cyprus have the strongest stagnation. In summer, also the Balearic region and the surrounding of the Italian peninsula have a tendency towards increased stagnation. Recirculation results show little spatial variability and certain features that are not easily understandable.

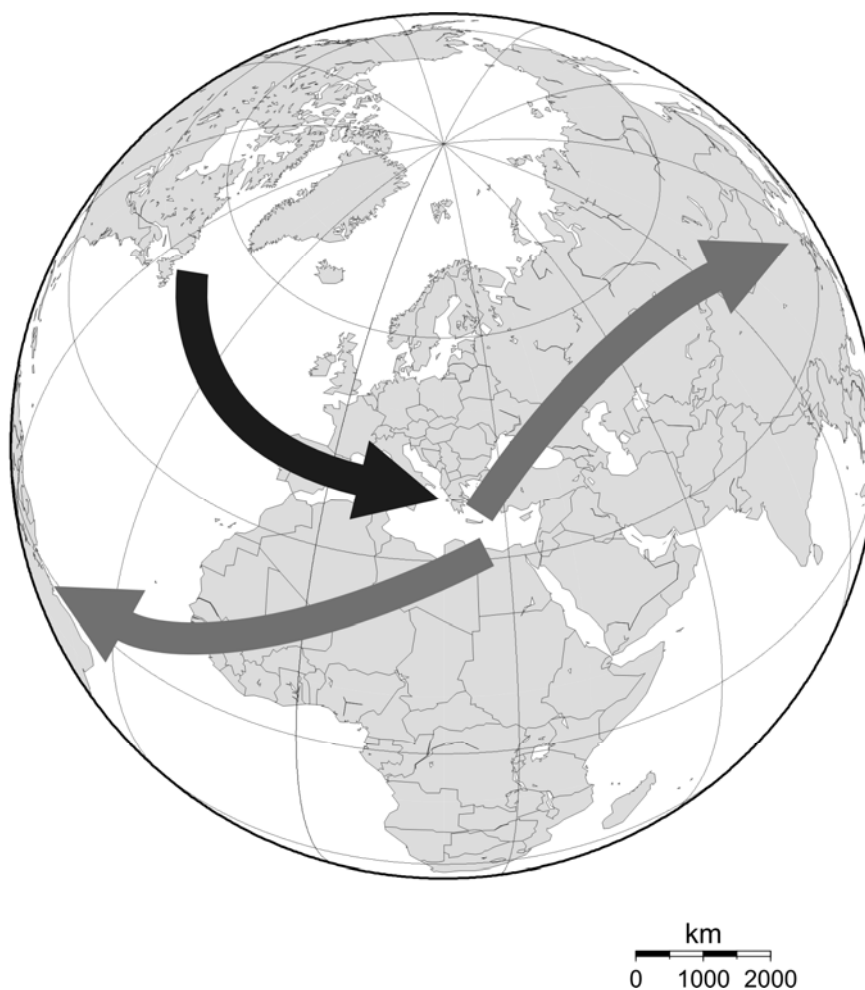


Figure 1: Air streams to (black) and from the Mediterranean (gray).

Additional map plots as well as numerical data can be obtained from BOKU on request.

---

## 2. Introduction

During the last several years studies have been carried out to evaluate moisture sources and sinks not only in the Mediterranean region but also in e.g. South America. Gallego et al. (2008) have tested different atmospheric dispersion models on their ability to evaluate atmospheric moisture sources for the Guadalquivir basin, Spain. Sodemann and Zubler (2007) used the LAGRANTO model to evaluate the origin of the precipitation in the Alps on a seasonal and inter-annual base. Stohl et al. (2008) used the Lagrangian particle model FLEXPART to trace back the origin of a heavy precipitation event in Norway in September 2005. Such evaluations were also carried out for a five year period (Stohl, 2006). He used a method developed and validated by Stohl and James (2004, 2005), also used by Nieto et al. (2006, 2007, 2008a) and Drumond et al. (2008). Sodemann et al. (2008) used a similar method for evaluating the precipitation origin. These two methods have been inspired by a method developed by Wernli and Davies (1997), who used a Lagrangian-based method of analysis to examine the dynamics of extratropical cyclogenesis and applied it to a case study (Wernli, 1997).

There are of course many other studies investigating the Mediterranean basin. We should mention especially Mariotti et al. (2002), who analysed the Mediterranean hydrological cycle for a 50-year period, the "Hydrological cycle in Mediterranean Experiment" (HyMeX), and the "Mediterranean CLimate VARIability and Predictability" (Med-CLIVAR) project. Zecchetto and De Biasio (2007) investigated properties of the wind climate over the Mediterranean Sea such as steadiness from scatterometer data.

In a recent study, contributing to Research Line 6 of the Circe project, Nieto et al. (2008b), evaluated moisture sources for three Mediterranean Sea basins and seven continental basins surrounding the Mediterranean, for 10-day averages in backward and forward mode.

The main objective of this deliverable is the generation of an air moisture balance database for the Mediterranean and selected airsheds. In addition, evaluations of residence times, stagnation and recirculation – quantities which are relevant for air pollution issues – have been carried out.

---

### 3. Data

Data used to generate this deliverable have been obtained from Andreas Stohl (NILU) who generated the dataset for a study on transport into the Arctic (Stohl, 2006). It was created with a global, homogeneous, domain-filling simulation by the Lagrangian particle dispersion model FLEXPART (Stohl et al., 1998; Stohl and Thomsom, 1999; Stohl et al., 2005). In this simulation, a total of 1,398,801 particles were tracked during a 5.5-year period, starting on 27 October 1999 and ending on 1 May 2005. This includes the extreme precipitation in Central Europe in Summer 2002 and the extreme drought and heat in Summer 2003. The meteorological input used in the simulation was taken from the operational analysis and 3-h forecast at intermediate times (03, 09, 15, 21 UTC) of the European Centre for Medium-Range Weather Forecast (ECMWF). The temporal resolution of the meteorological data is 3-hourly, the horizontal resolution is  $1^\circ \times 1^\circ$  with 60 model levels in the vertical. Of these 60 levels, 14 are below 1500 m and 24 below 5000 m.

FLEXPART model output has been produced every 6 h with a dump of the particles' properties as follows:

- particle ID number for tracking single particles
- particle position (latitude, longitude, height above msl, and height above ground)
- a set meteorological parameters: temperature  $T$ , specific humidity  $q$ , air density  $\rho$ , atmospheric boundary layer (ABL) height at the particles' position and the tropopause height at the particles' position.

The resolution of the input data implies that meso- $\beta$  and  $\gamma$ -scale circulations are not resolved. In addition to this, one particle represents about  $3E12$  kg or a volume of  $150 \text{ km}^2 \times 20 \text{ hPa}$  (a total air mass of  $5E18$  kg). Therefore, case studies are not possible and an averaging of the results over many particles is needed. Results are presented on a seasonal and annual base.

In addition to the FLEXPART dataset, a land-sea mask obtained from the ECMWF in  $1^\circ \times 1^\circ$  resolution (Figure 2:) has been used to stratify the results into particles over land and over water.

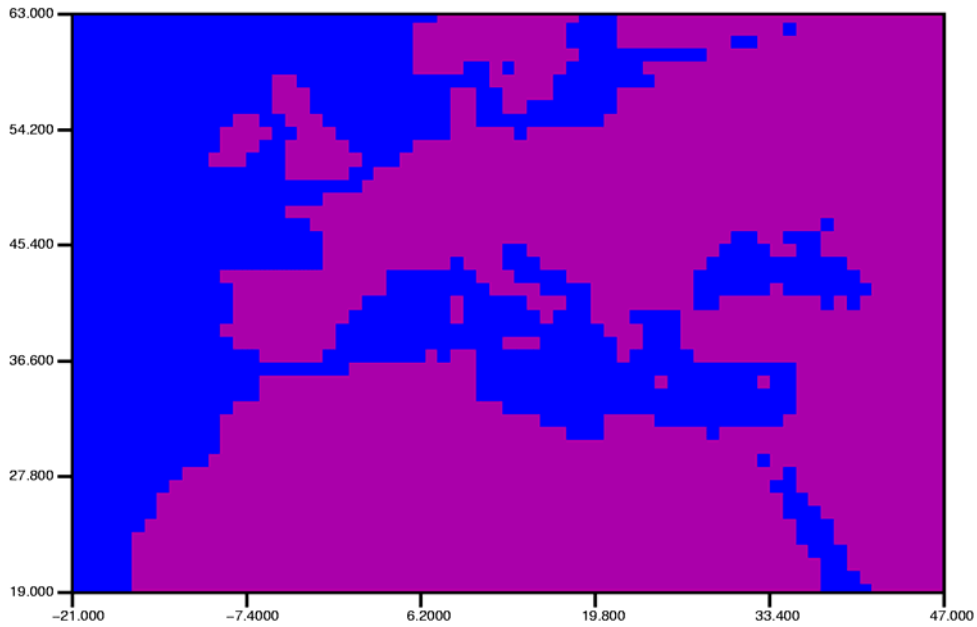


Figure 2: Land-Sea mask for the Mediterranean in a 1° x 1° resolution as used in this study.

## 4. Definition of Regions of Interest

The first step was defining our Region Of Interest (ROI). The Mediterranean is a region encapsulated by straits and by mountain ridges in the North as well as in the South, East and West and is greatly influenced through local or regional wind systems such as the bora, the ponent, the scirocco or the etesians. Therefore, we decided to consider the regions of these characteristic flows in the definition of our ROIs.

The Mediterranean basin is naturally divided into four large basins (Figure 3.): Western Mediterranean (1), Central Mediterranean (2), Eastern Mediterranean (4) and the Adriatic Sea (3). In addition, three sub-regions have been defined: the Etesian (6), the Balearics (5), and a region between Cyprus and Israel (7). Analyses have been carried out for these seven ROIs and the whole Mediterranean Basin.

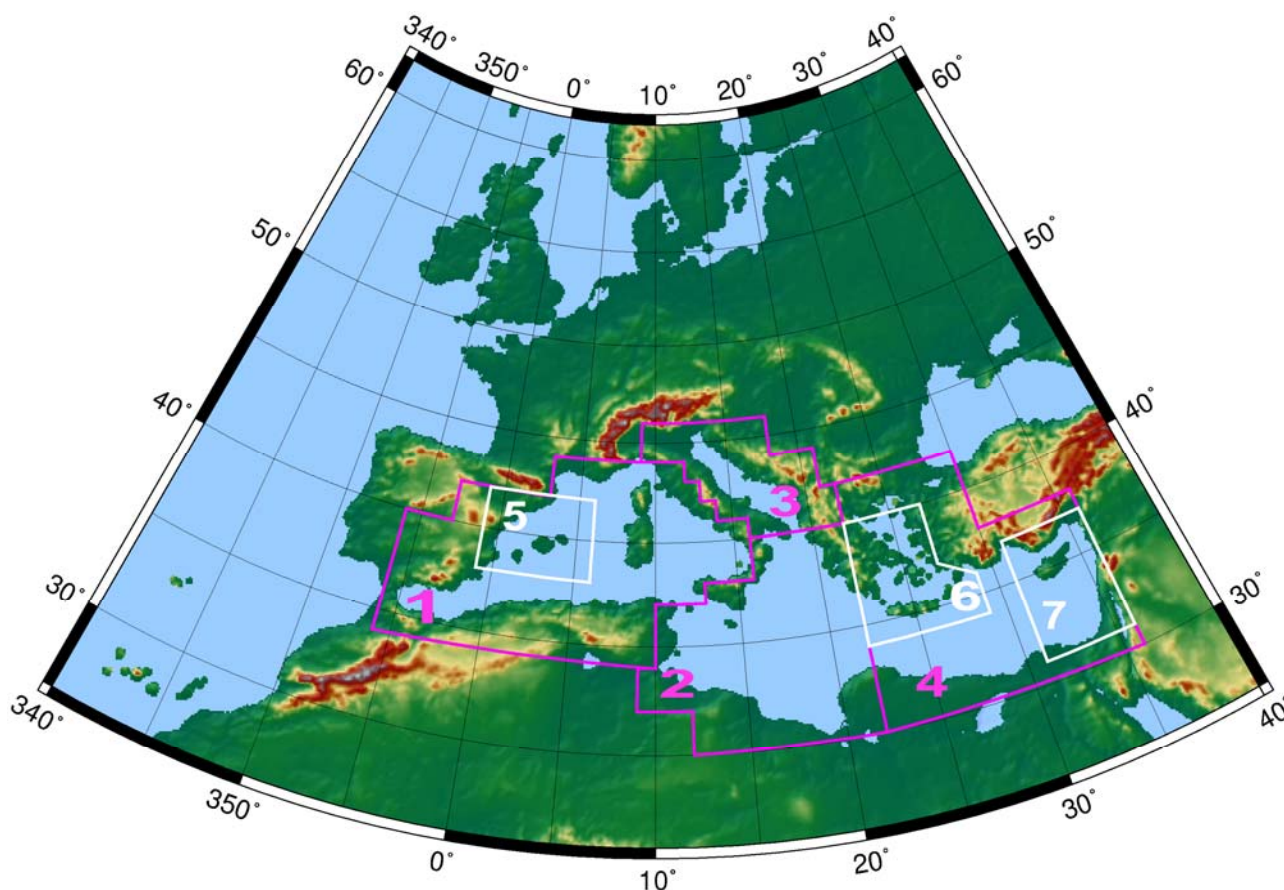


Figure 3: Definition of the sub-basins used. 1 Western Mediterranean, 2 Central Mediterranean, 3 Adriatic Sea, 4 Eastern Mediterranean, 5 Balearics, 6 Etesian, 7 Cyprus.

## 5. Moisture and Precipitation Budgets

### 5.1. Moisture budget and moisture flux

Moisture source and sink tracking along the trajectories has been done using a method based on James et al. (2004); Stohl and James (2004, 2005), and Sodemann (2006); Sodemann et al. (2008a,b), also used by Nieto and Gimeno (2006); Nieto et al. (2006, 2007, 2008) and Drumond et al. (2008).

The change of moisture in an air parcel  $n$  between a time interval,  $\Delta q_n / \Delta t$  can be written as the net result of evaporation  $E$  minus precipitation  $P$ :

$$\frac{\Delta q_n}{\Delta t} = E - P \quad (1)$$

Evaluations are carried out on a fixed 6-h time interval. Results of  $\Delta q_n$  have units of  $\text{g kg}^{-1}(\text{6 h})^{-1}$ . The moisture change between two time steps is calculated as  $\Delta q_n = q_n(t) - q(t-1)$ , where  $q_n(t)$  is moisture at time  $t$  and  $q(t-1)$  is the moisture at the previous time step.

In order to distinguish between moisture originating inside and outside the ROIs, two different moisture variables are defined. We track moisture originating inside the ROIs,  $qm_n$ , with its changes between the timesteps,  $\Delta qm_n$ , and moisture originating outside the ROI,  $qo_n$ , with changes  $\Delta qo_n$ .

An increase of  $qm_n$  is found if  $\Delta q_n$  is positive and if the particle is inside the ROI, with

$$\Delta qm_n = \Delta q_n \quad (2)$$

where the moisture originating outside the ROI does not change:

$$\Delta qo_n = 0 \quad (3)$$

If the particle is outside of the ROI,  $\Delta qo_n = \Delta q_n$  and  $\Delta qm_n = 0$ .

With a decrease of a particle's moisture between two timesteps (negative  $\Delta q_n$ ), both  $qm_n$  and  $qo_n$  loose moisture pro-rata. In this case,  $\Delta qm_n$  and  $\Delta qo_n$  can be calculated as:

$$\Delta qm_n = \frac{qm_n}{(qm_n + qo_n)} \Delta q_n$$

$$\Delta qo_n = \frac{qo_n}{(qm_n + qo_n)} \Delta q_n$$

(4), (5)

The fraction of the total moisture which evaporated inside the ROI,  $qm_i(x,y)$ , can be written as:

$$qm_i(x,y) = \sum_n \frac{qm_n}{(qm_n + qo_n)} \quad (6)$$

with

$$qm_n = \sum_n \Delta qm_n \quad (7)$$

and

$$qo_n = \sum_n \Delta qo_n \quad (8)$$

where  $n$  are the particles in the gridbox. This fraction  $qm_i(x,y)$  is then averaged over the seasons, and averaged over  $1^\circ \times 1^\circ$  grid boxes. Note that each particle represents a defined, constant fraction of the total atmospheric mass, and density effects are represented by the particle density. Thus the air density does not appear in these equations.

In the ABL, moisture may change along a computational particle's trajectory by turbulent displacements in an environment that -- according to the ECMWF input fields used by the original FLEXPART calculation and interpolations made therein -- has a vertical specific moisture gradient without occurrence of evaporation or precipitation. Such effects would cause a too fast loss of Mediterranean moisture outside the ROI and of non-Mediterranean moisture inside the ROI. To counter this, the specific humidity of all particles inside the ABL is set to the average value over all the particles below ABL height and in the respective  $1^\circ \times 1^\circ$  grid box. Furthermore, in the calculation of  $\Delta q_n$ , each specific humidity value is replaced by the average between the present and the previous time step. It should be noted that Mediterranean moisture may still decrease faster in the model than in reality and absolute values thus may be underestimated.

In addition to the mixing ratio of the two kinds of moisture, vertically integrated horizontal fluxes of moisture  $F_{qn}$  originating in the Mediterranean basin (Fig. \ref{f-rios}) were calculated. The flux associated with a single particle is

$$\mathbf{F}_{qn} = \mathbf{v}_n \overline{qm_n} M_p \quad (9)$$

where the horizontal velocity vector  $\mathbf{v}_n$  is taken from the particle displacement and

$$\overline{qm_n} = qm_n(t-1) + \frac{qm_n(t) - qm_n(t-1)}{2} \quad (10)$$

The mass of air represented by each particle is the total atmospheric mass ( $5.1 \times 10^{18}$  kg divided by the total number of particles, i.e.  $3.65 \times 10^{12}$  kg).

The gridded flux vector  $F_q$  is obtained by summing up all the  $F_{qn}$  in  $1^\circ \times 1^\circ$  horizontal grid cells and vertically between 0 and 1000~m and between 0 and 20000~m agl divided by the area of the grid cell. It is thus expressed in units of  $\text{kg (m s)}^{-1}$ , signifying the amount of Mediterranean moisture being transported across a line of 1 m length in 1 s.

## 5.2. Mediterranean moisture budgets

Seasonally averaged values of  $qm_i(x,y)$  (i.e., the fraction of moisture evaporated inside the ROI) were calculated for eight ROIs. Results for the Mediterranean basin as a whole (Figure 4:) show that the highest fractions of moisture are formed over the basin itself with the centre located between the Italian and Hellenic peninsulae. These structures of the moisture fraction  $qm_i(x,y)$  are present in all four seasons, especially in the three summer months June, July, and August (in the following JJA) where two centres with values between 9 % and 11 % evolve. One centre is located with the maximum at the coast of Tunisia, covering part of the western Mediterranean basin and the central Mediterranean basin. The other one is located between the south coast of Turkey and Cyprus. In autumn and winter, when the evaporation from the sea is large due to high SST compared to air temperature, and advection is strong,  $qm_i(x,y)$  contributes with fractions of 1.5 % and more to regions outside the Mediterranean and to a lower extent in spring and summer. Contributions of up to 4 %, except for summer with lower values of maximum 2.5 %, even reach Kazakhstan and European Russia. The coastal areas of Egypt, Libya and Tunisia experience up to 8 % of Mediterranean moisture, showing the relevance of the Mediterranean for these areas.

In the main outflow region following the westerlies in the northeastern part of the Mediterranean,  $qm_i(x,y)$  shows some influences inland, e.g. in Turkey, the Levant, and Bulgaria with up to 6 % in regions close to the Mediterranean coast and still up to 3 % in the other regions. Mediterranean moisture can be found, although with a very low fraction of less than 0.1 %, in the whole northern hemisphere. The spatial distribution of  $qm_i(x,y)$  mainly reflects the predominant transport pathways in the corresponding seasons. Moisture transport to the northeast is strong especially in SON and DJF due to the SST effect.

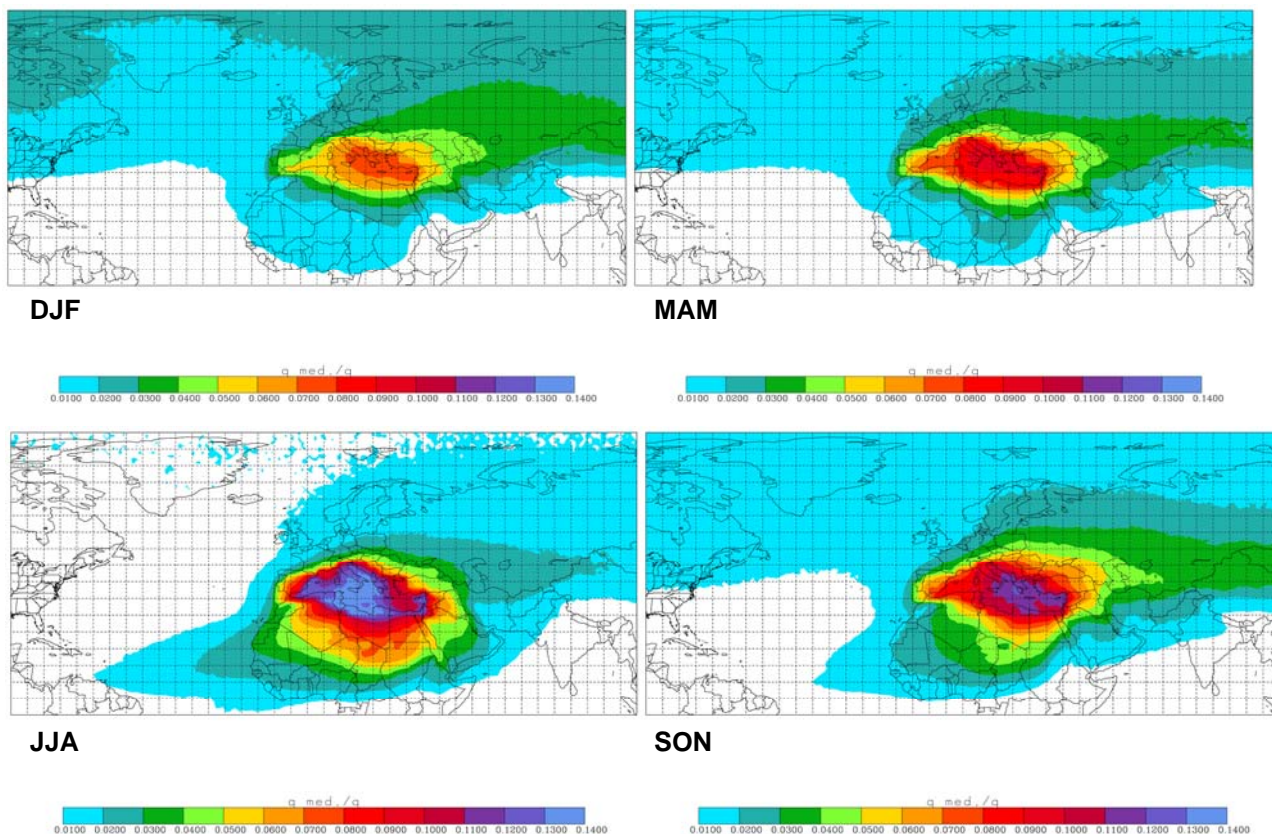


Figure 4: Mixing ratio of Mediterranean moisture and moisture outside the Mediterranean for the four seasons.

The aforementioned pathways and flows, which could already be seen to a certain extent in the moisture budget analyses and in the residence time analyses, are clearly identifiable in the moisture flux analysis in Fig. 4 for the 0-20000 m height interval. Pathways of Mediterranean moisture show ingestions into the ITCZ in all seasons. Strongest flux is found in JJA with three separate flows: one flow over Egypt with  $70 \text{ kg (m s)}^{-1}$ , the second one over Libya with  $125 \text{ kg (m s)}^{-1}$ , and the third one goes over the Gulf of Gabès and Tunisia with up to  $50 \text{ kg (m s)}^{-1}$ . Outflow into the Red Sea is strongest in JJA with maximum  $50 \text{ kg (m s)}^{-1}$ . Mesopotamia receives up to  $125 \text{ kg (m s)}^{-1}$  showing the relevance of the Mediterranean for this region. Over the Arabian peninsula another path into the ITCZ is present. Recirculation tendencies between the Balearics and the southern coast of Spain are visible in the lowest 1000 m (not shown here). In SON, DJF, and MAM a southerly flow in the Adriatic basin can be found showing the presence of the Sirocco. Results for the 0-20000 m moisture flux evaluations show similar paths as the lowest 1000 m (not shown) but with higher flux values. Small scale features such as the northerly flow in the Adriatic basin and the recirculation on the southeastern shore of the Iberian peninsula are overlaid whereas the influences of the mountainous regions are still visible.

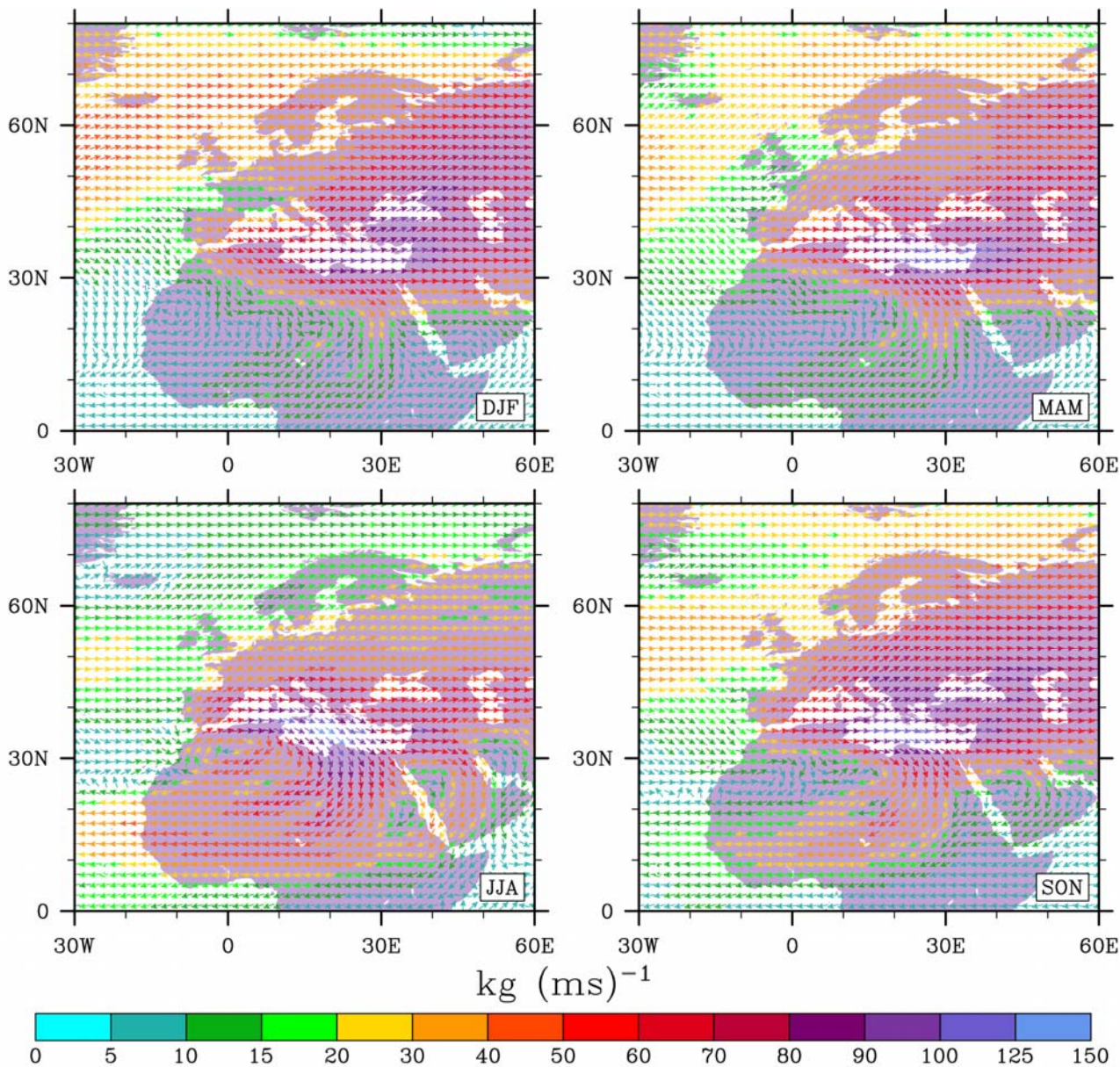


Figure 5: Calculated moisture flux for particles crossing the Mediterranean basin. For visibility, only every second grid point in x and y direction is plotted. Moisture fluxes are shown for the vertical layer below 20000m.

### 5.3. Moisture budget of sub-basins

#### Western Mediterranean

The outflow of moisture from the western Mediterranean (Figure 6:) is directed primarily to the northeast and east contributing to precipitation in these areas. Especially in autumn, contributions of the western Mediterranean basin reach 2-3 %, i.e. on the southern slopes of and in the Alpine region. Sodemann and Zubler (2010) showed that the western Mediterranean sector, covering in our definition ROI 1 and ROI 2, plays a major role for Alpine precipitation throughout the seasons, but especially in August and September, again related to ocean evaporation. In summer, we see minor ingestion into the trade wind regime through the Strait of Gibraltar, and into the ITCZ through Algeria and Libya, contributing with up to 8 % to the coast of Algeria and Libya during the summer season.

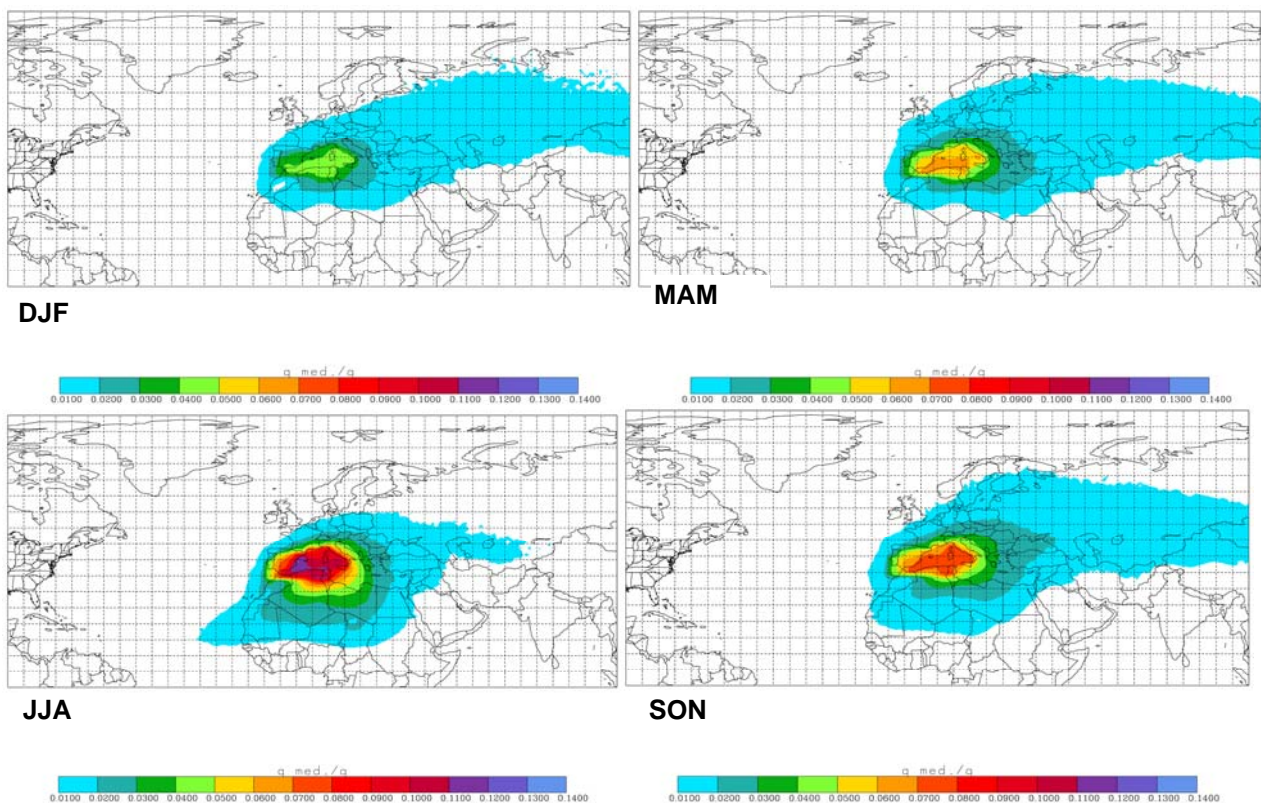


Figure 6: Fraction of moisture from Western Mediterranean basin for the four seasons.

### Central Mediterranean

The moisture uptake in the central Mediterranean (Figure 7:) has only weak influences on regions outside the Mediterranean, partially because the basin is smaller. Although the influences are small, there are still contributions up to 1.5 % close to the northern border of Chad in summer. The main input to the surrounding areas of the basin is into the northeast.

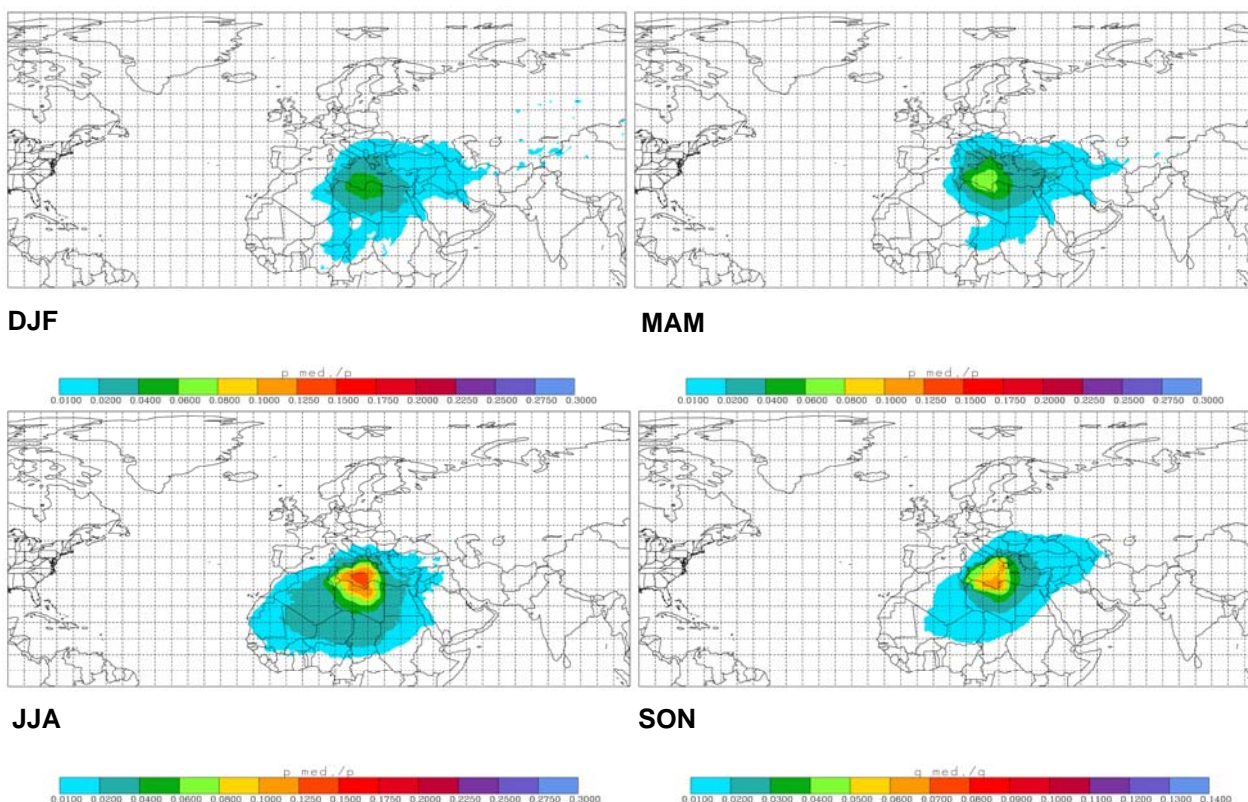


Figure 7: Same as Figure 6: but for the Central Mediterranean basin.

### Eastern Mediterranean

The Eastern Mediterranean (Figure 8:) contributes its moisture to the region itself and the whole Near East. Only little influence, below 1.5 %, is found in areas further to the east and south. Especially the coastal area of the Levant receives up to 6 % of the Eastern Mediterranean moisture in summer, and 5 % during the other seasons. has weak influences on regions outside than that of other Mediterranean regions, at least partially because the ROI is smaller. In summer, the region with up to 20% moisture from the ROI reaches close to the northern border of Chad. The main other outflow pathway, dominant in the other three seasons, is towards the northeast. There is no relevant outflow through the Strait of Gibraltar. The maxima are once more found in the southern part of the ROI itself.

Predominant outflow is on one hand towards the east, on the other hand southward into the ITCZ. The Eastern Mediterranean influence reaches further south than that of any other major basins, and it is present in all seasons, being strongest in spring and autumn. No moisture is transported westwards, and little is going north.

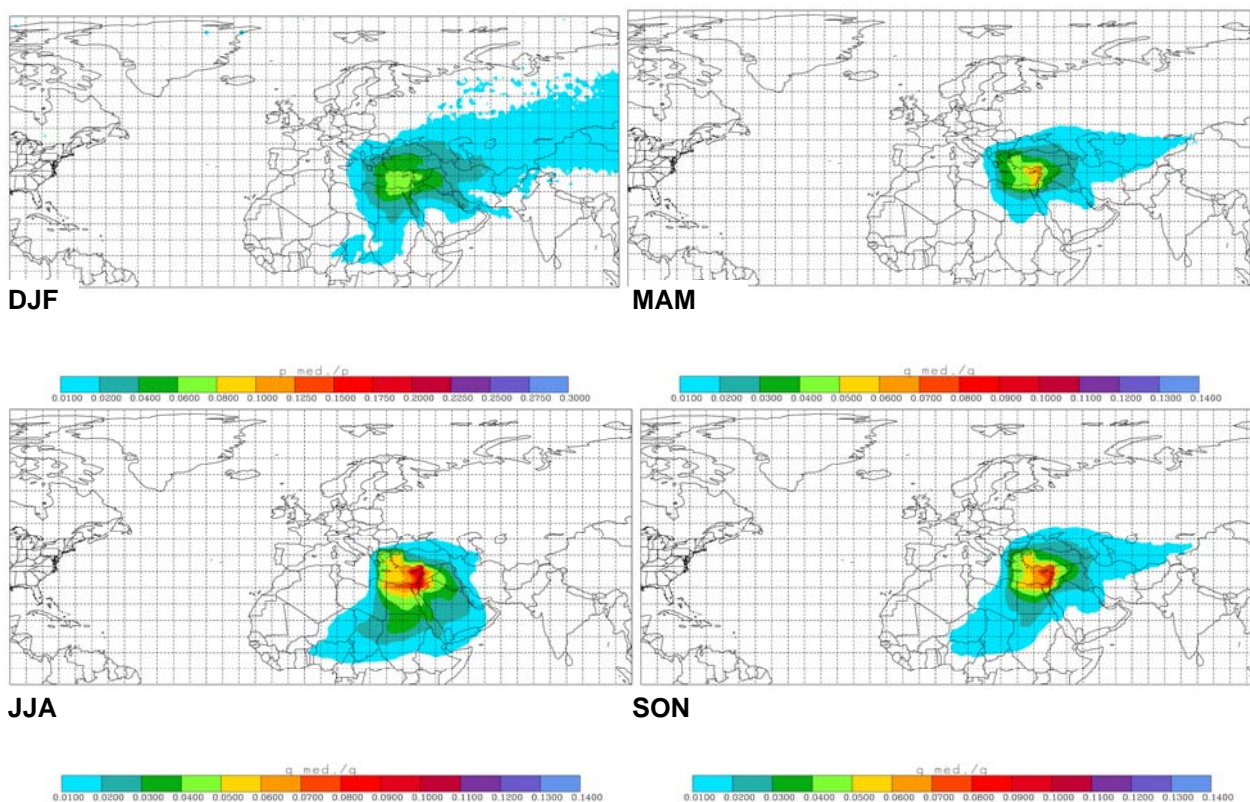


Figure 8: Same as Figure 6: but for the Eastern Mediterranean basin.

## Balearic

The Balearic basin moisture mixing ratio (Fig. 9) contributes 5 % in summer and 1-3 % in the other seasons to air moisture above the Iberian peninsula. This shows that the thermal circulation between the Balearic Sea and the Iberian continent is represented to some extent even in the coarse ECMWF model. Some minor influence of the Balearic basin moisture, between 0.5 % and 1.5 %, is found over the Italian peninsula. This influence is strongest in summer while being present, although weaker, in the other seasons, too.

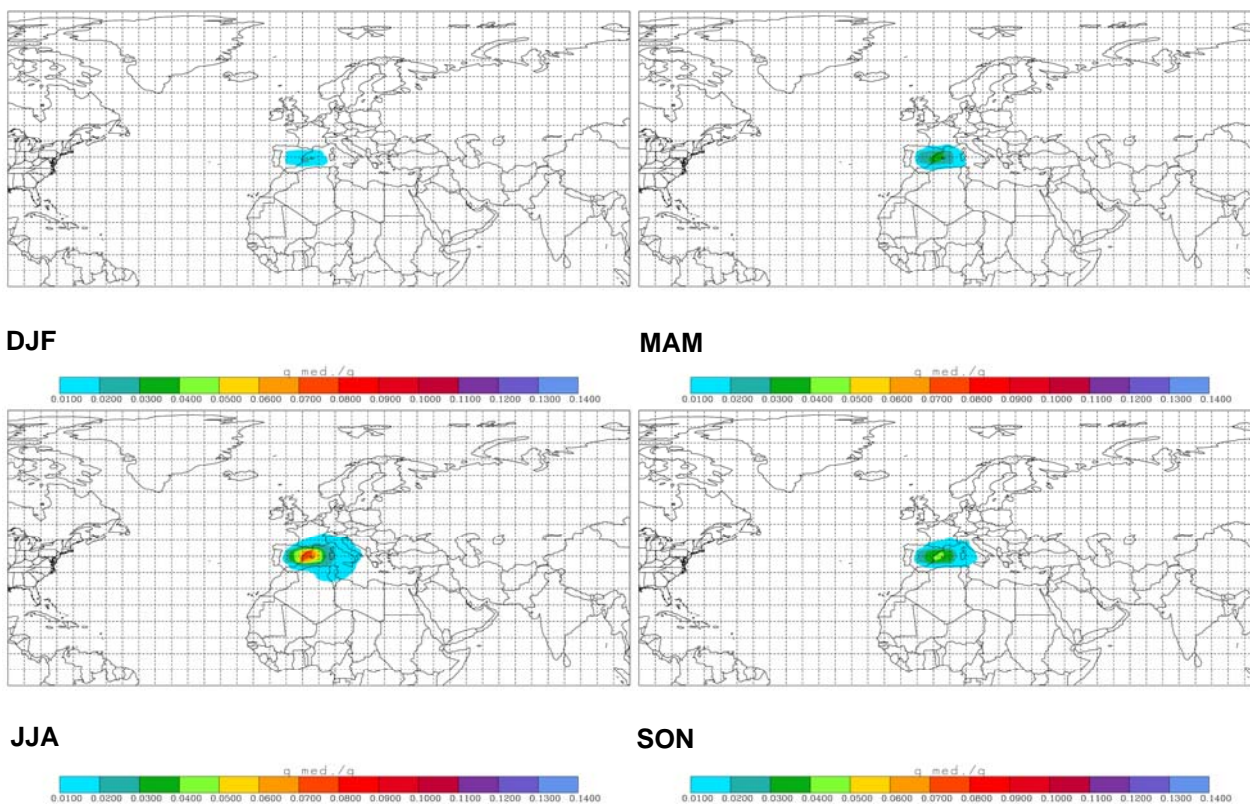


Figure 9: Same as Figure 6: but for the Balearics.

### Adriatic Sea

The Adriatic basin, ROI 3 (Figure 10:), shows more influence on the western part of the Balkan than on Italy. A closer look reveals that that the Po basin has a significant moisture fraction of up to 4 % originating in the Adriatic, and the existence of a strong gradient over the western Alps. Up to 4 % in summer and 3 % in the other seasons of the Adriatic moisture is present at the Balkan coast. Switzerland receives virtually no Adriatic moisture whereas southern and eastern Austria do, although with a small amount of up to 2 %.

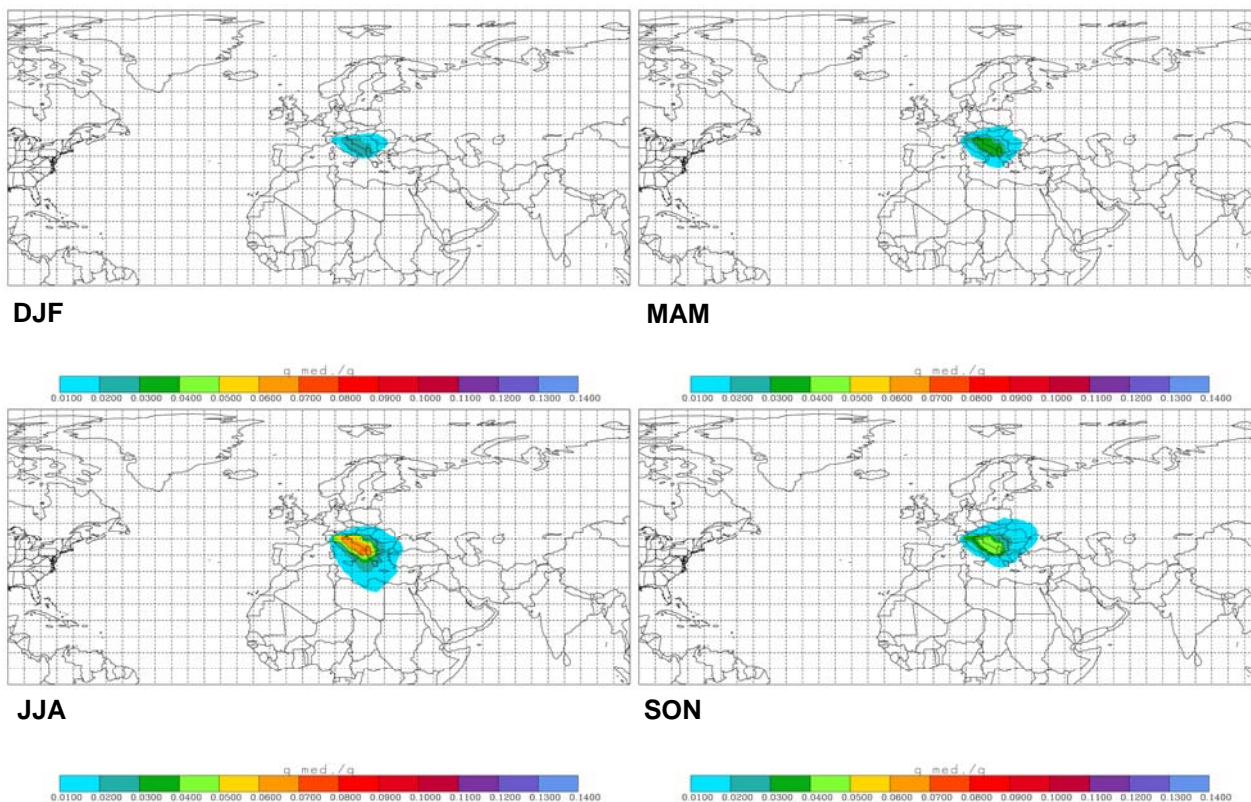


Figure 10: Same as Figure 6: but for the Adriatic Sea.

## Etesian

In the Etesian basin, the contribution of Mediterranean moisture is distributed locally with small fractions below 2 % in the area of the Black Sea and Turkey in the northeast in winter and spring, and the Sahara region in summer and autumn.

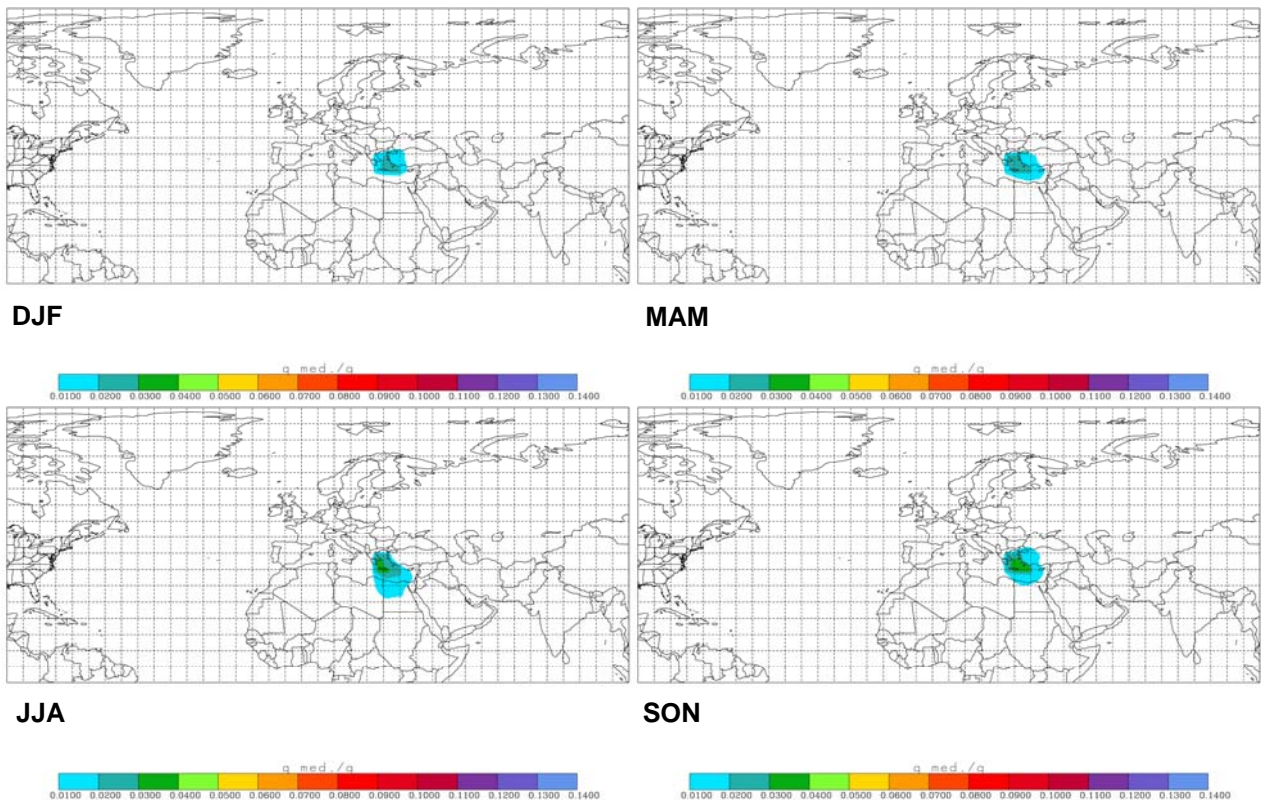


Figure 11: Same as Figure 6: but for the Etesian basin.

## Cyprus

The Cyprus basin has results similar to the Aegean but with flow directions to the east and southeast and higher fractions of Mediterranean moisture. Fractions of Mediterranean moisture can be found in the region between the Eastern Mediterranean shoreline and Iraq. In contrast to the Aegean, shallow flows of the moisture originating from the Cyprus basin are sucked into the atmosphere over Africa.

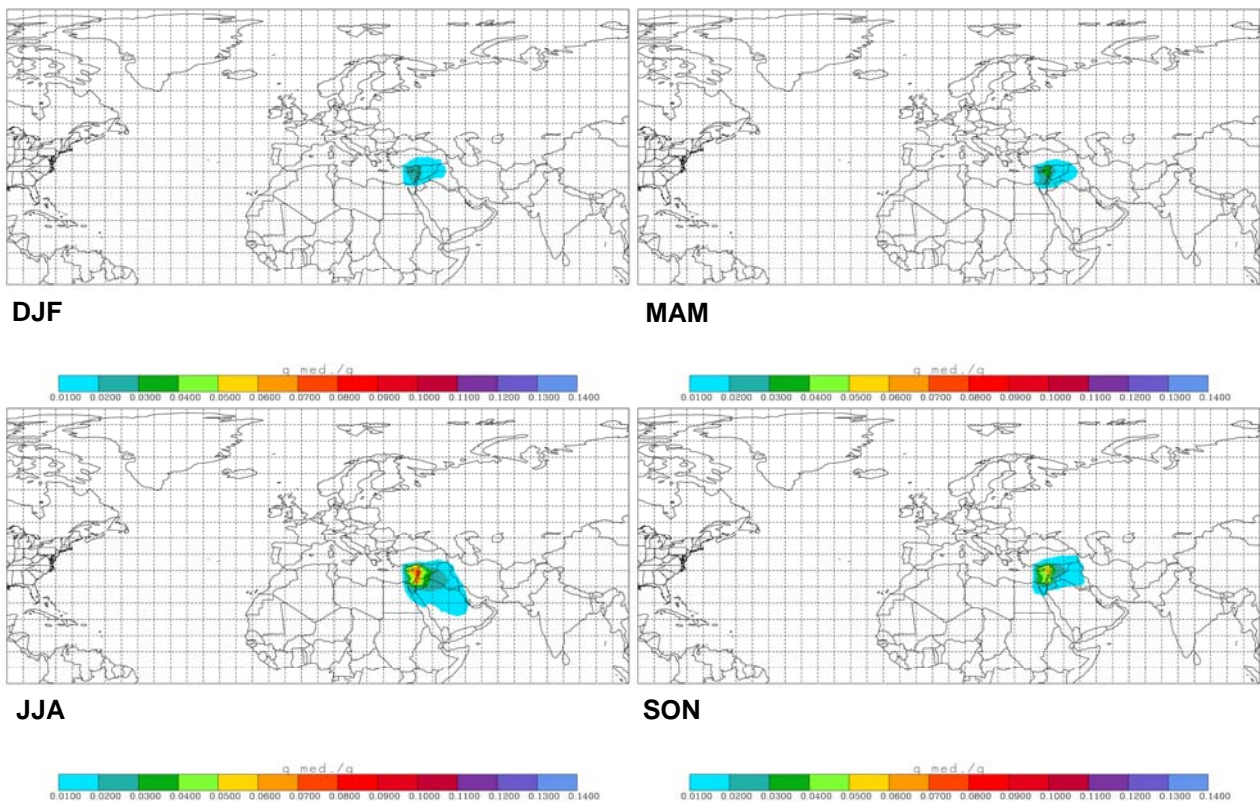


Figure 12: Same as Figure 6: but for the Cyprus basin.

#### **5.4. Methods for evaluation of precipitation budgets**

The attribution of precipitation with respect to its origin in the ROIs was done in a similar way as the moisture calculations. The moisture changes inside and outside the ROI are evaluated and the moisture loss in the atmospheric column is calculated and considered to represent precipitation.

A precipitation fraction  $p_m(x,y)$  is calculated in a similar way as before the moisture fraction, but instead of  $\Sigma qm_n$  and  $\Sigma qo_n$ , the quantities  $\Delta qm$  and  $\Delta qo$  as defined in Eq. 3 are used. Then,  $p_m(x,y)$  is obtained as:

$$p_{m_i}(x, y) = \sum_n \frac{\Delta qm_n}{(\Delta qo_n + \Delta qm_n)} \quad (1)$$

This value indicates the fraction of the precipitation on a grid cell that stems from moisture which evaporated from the ROI. In the interpretation, it has to be considered that a small ROI will of course contribute less moisture to any precipitation downwind than a larger ROI.

#### **5.5. Precipitation budgets of the Mediterranean as a whole**

In the Mediterranean basin (Figure 13:) the fraction of autochthonous precipitation is at least 14 % throughout the year. In summer it is highest, with values between 20 % and 28 %, showing quite sharp edges compared to the other seasons. Seasonal results show, like in the moisture analyses, the influence of the higher SST in autumn compared to spring. In autumn, a maxima of 24 % is located in the eastern Mediterranean. Outflow pathways can be clearly identified, having one strong branch towards the northeast, and a second, weaker one, towards central Africa, especially to the eastern part of the continent. Western North Africa receives less Mediterranean rainwater. Anker et al. (2007) identified in the Jordan Rift Valley six air pathways for precipitation events. They found that the chemical composition of the precipitated water of the western trajectory is associated purely marine thus originating from the Mediterranean Sea. A third maximum is found in the region of Gibraltar, reaching into the trade wind zone in summer, although with a very low fraction. A fourth maximum is found over eastern Central Europe in spring and autumn, probably related to the well-known higher frequency of meridional circulations in these seasons (Seibert et al., 2006) connected with Vb-like cyclone tracks (Van Bebber, 1891).

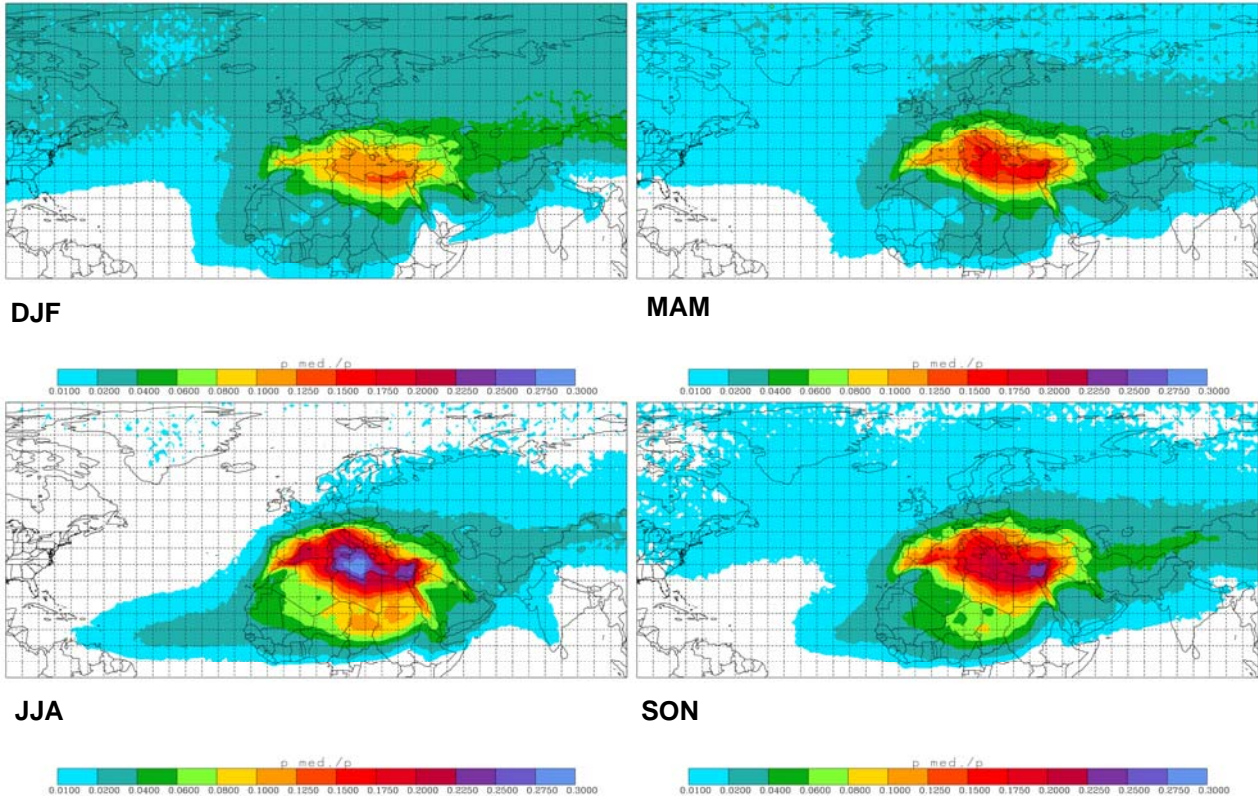


Figure 13: Mixing ratio of the precipitation originating in the Mediterranean to the total precipitation for the four seasons.

## 5.6. Precipitation budgets of sub-basins

### Western Mediterranean

Precipitation originating in the western Mediterranean basin (Figure 14:) contributes to the precipitation at the Algerian and Tunisian coast, the Balearics and southern Sardinia, especially in summer. In summer, a strong gradient in the north of the basin across the Alpine region is visible. Also a weak transport into the trade wind zone is present. In autumn and winter, when precipitation originating in the western Mediterranean reaches into Central Asia, the influences in the north east are larger than in summer. In Iberian peninsula, this value higher in spring, summer, and autumn with up to 12 % of precipitation originating in the Mediterranean. Except for winter, precipitation originating in the Western Mediterranean basin is present over the Adriatic Sea and Italy.

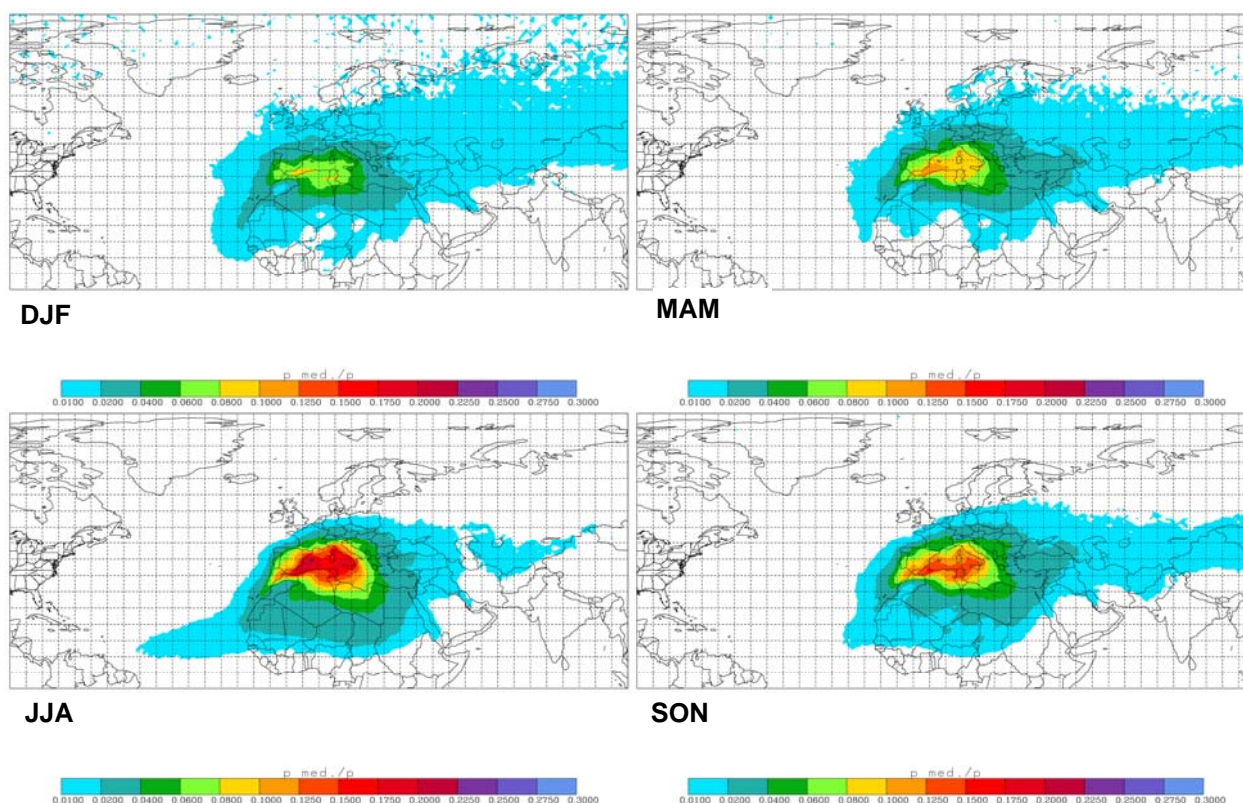


Figure 14: Mixing ratio of the precipitation originating in the Western Mediterranean basin and other precipitation origin shown for the four seasons.

## Central Mediterranean

Influence of precipitation originating in the central Mediterranean (Figure 15:) is changing little over the seasons. In summer and autumn, transport into northern Africa is visible, influence to the northeastern areas is strongest in winter and autumn.

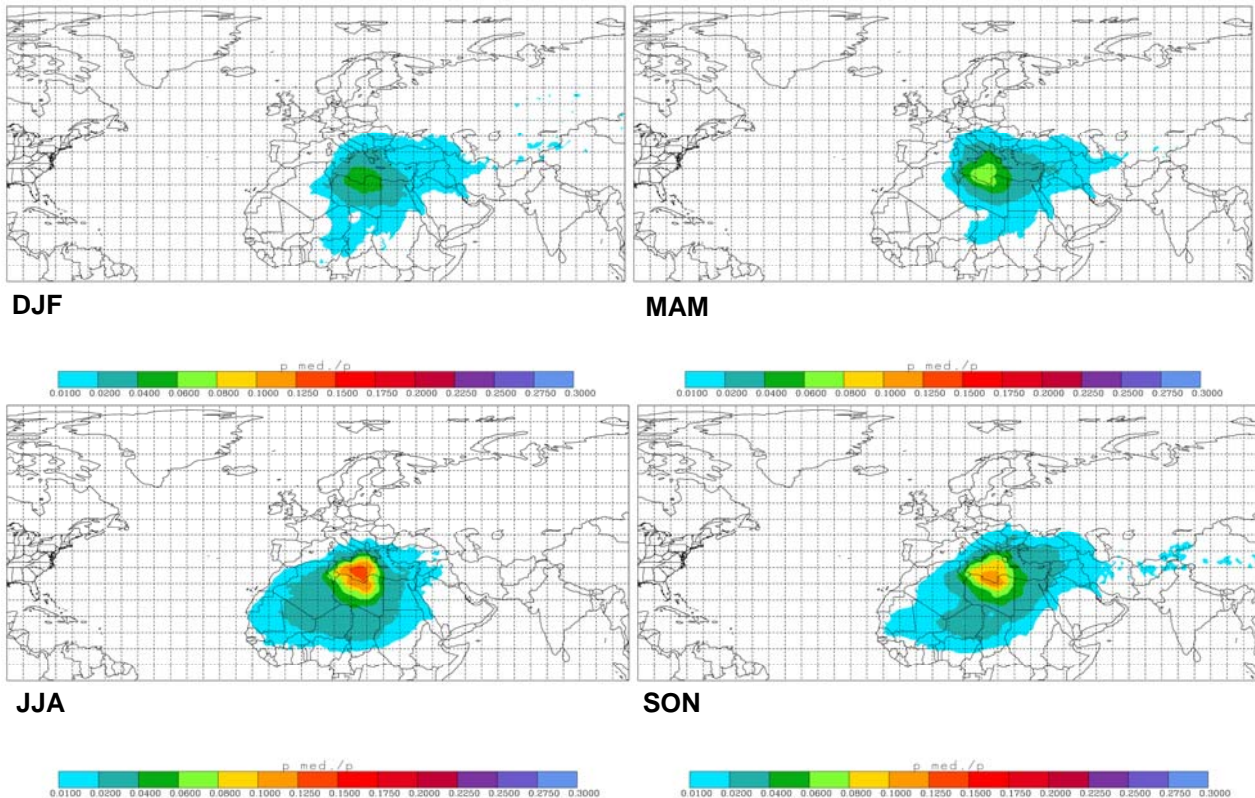


Figure 15: Same as Figure 14: but for the Central Mediterranean basin.

### Eastern Mediterranean

The eastern Mediterranean basin (Figure 16:) show the influence of the basin to the surrounding land mass. During spring, summer, and autumn contributions of the basin to the precipitation in Cyprus are within the range between 16 % to 20 %, in winter the contribution is between 4 % to 8 %. In summer and autumn the coasts of Egypt, Turkey, Israel, Lebanon, Jordan, and Syria receive 4 % to 12 % of precipitation. Influences of moisture originating in the eastern Mediterranean basin can be found in the precipitation during all seasons reaching far into the land masses with up to 4 %, showing distinct transport pathways. Influence of the westerlies are large in winter, spring and autumn. Small contributions can be found in the northwest of Chad in the Tibesti mountains where the precipitation originating in the Mediterranean is below 4 % but still visible in the north, east, and south of the mountain ridges.

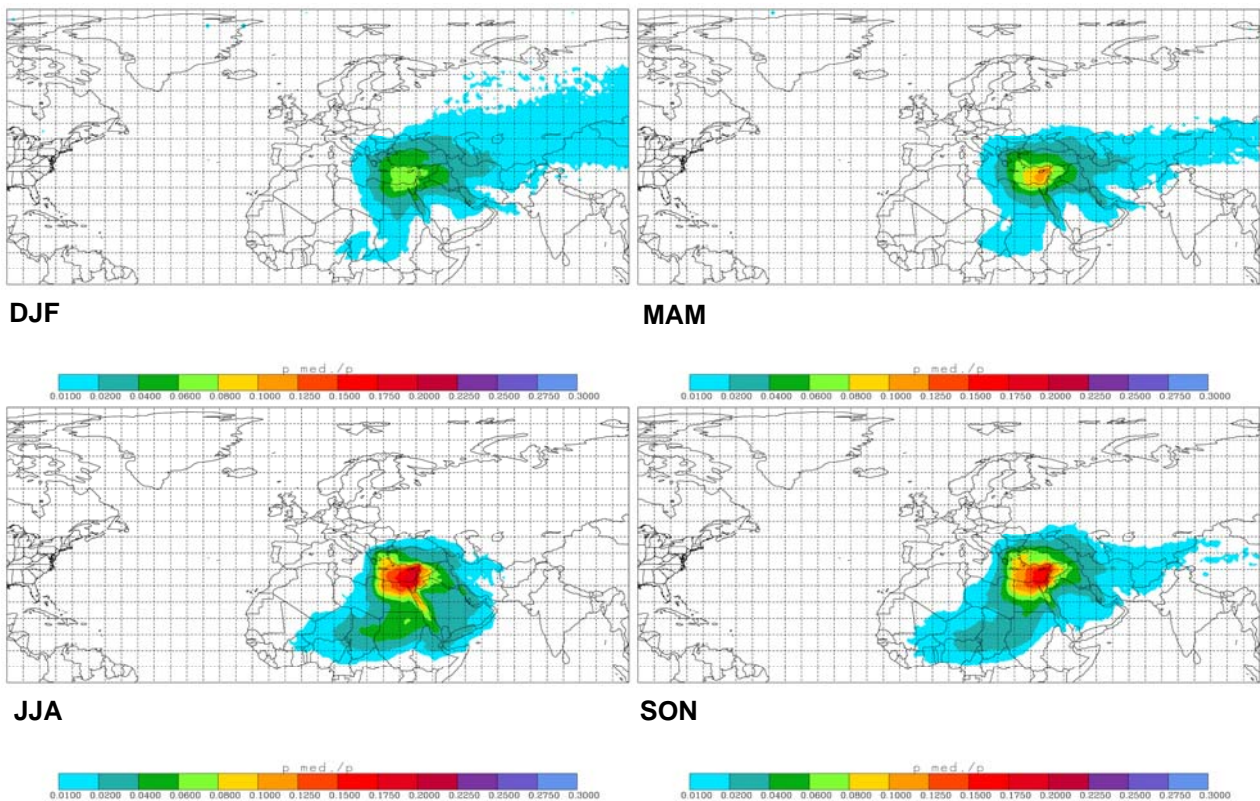


Figure 16: Same as Figure 14: but for the Eastern Mediterranean basin.

### Balearics

Precipitation originating in the Balearic basin (Figure 17:) influences, in summer, the region most strongly between the Balearic islands and the coast of Valencia. Contributions are also present in the Alpine region in southern France, except for winter. Cyclones in the western Mediterranean are known to cause heavy precipitation in these regions, and a substantial fraction of this water comes from the Balearic sub-basin. Transport with the trade winds and with the westerlies is almost absent in the Balearic precipitation budget.

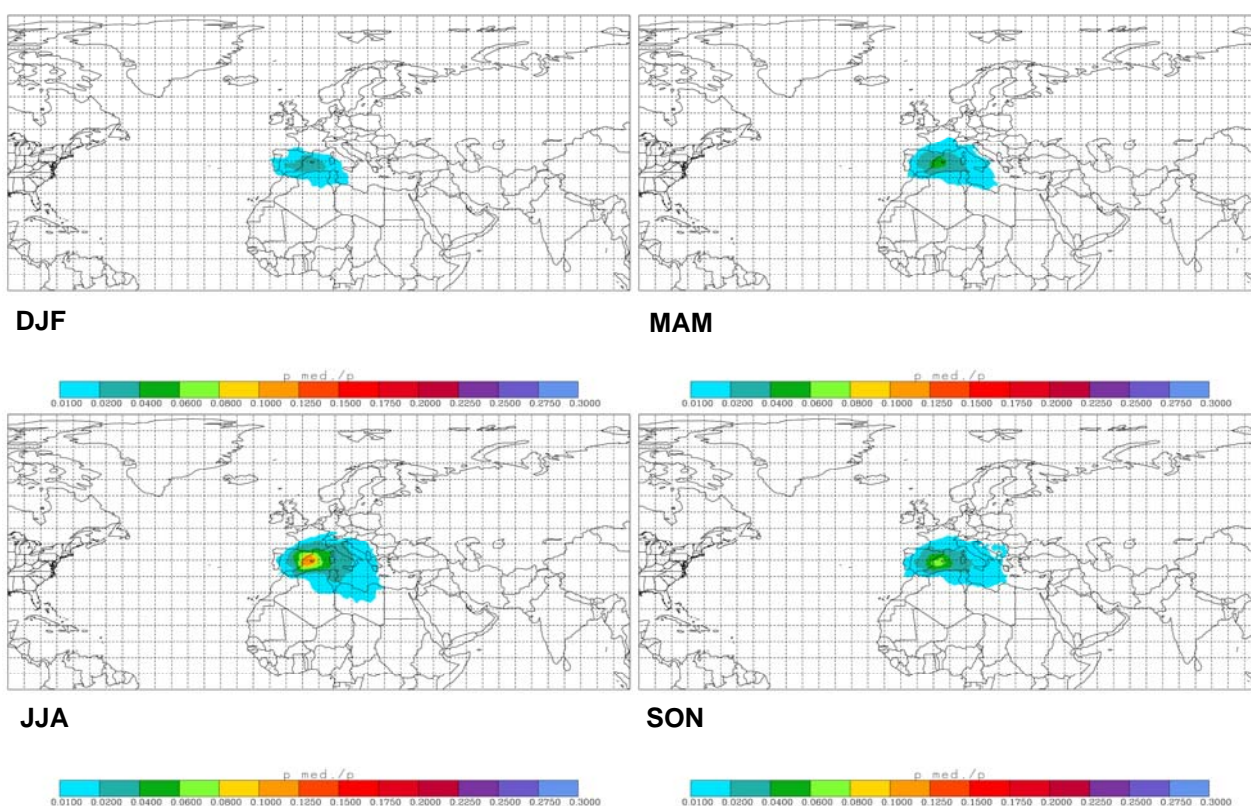


Figure 17: Same as Figure 14: but for the Balearics.

### Adriatic Sea

Similar to the results of the Balearic basin, the Adriatic Sea basin precipitation (Figure 18:) influences are only local. Fractions are highest in the southern Adriatic Sea, especially in summer. In contrast to moisture, the Po Basin in northern Italy is not a feature for precipitation. Among the land areas, the Dinaric coast has the highest fraction of Adriatic water in precipitation. However, in the main precipitation season (autumn), the fraction is only about 8 %, what reveals that sources of atmospheric moisture from more distant areas contribute as well.

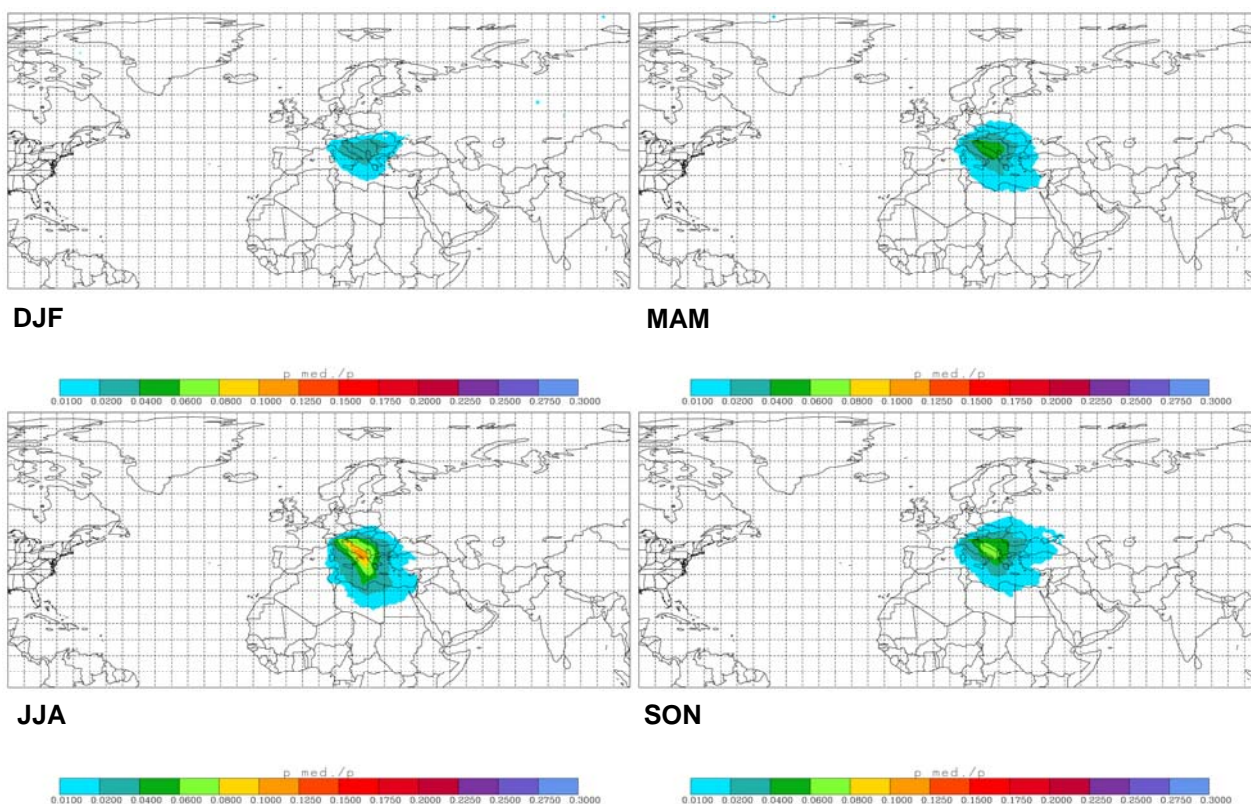


Figure 18: Same as Figure 14: but for the Adriatic Sea.

## Etesian

Again, precipitation originating from this sub-basin is mostly relevant in the ROI itself (Figure 19:). The 2 % zone reaches into Egypt with the trade winds in summer, in winter transport with the westerlies comes close to Crimea.

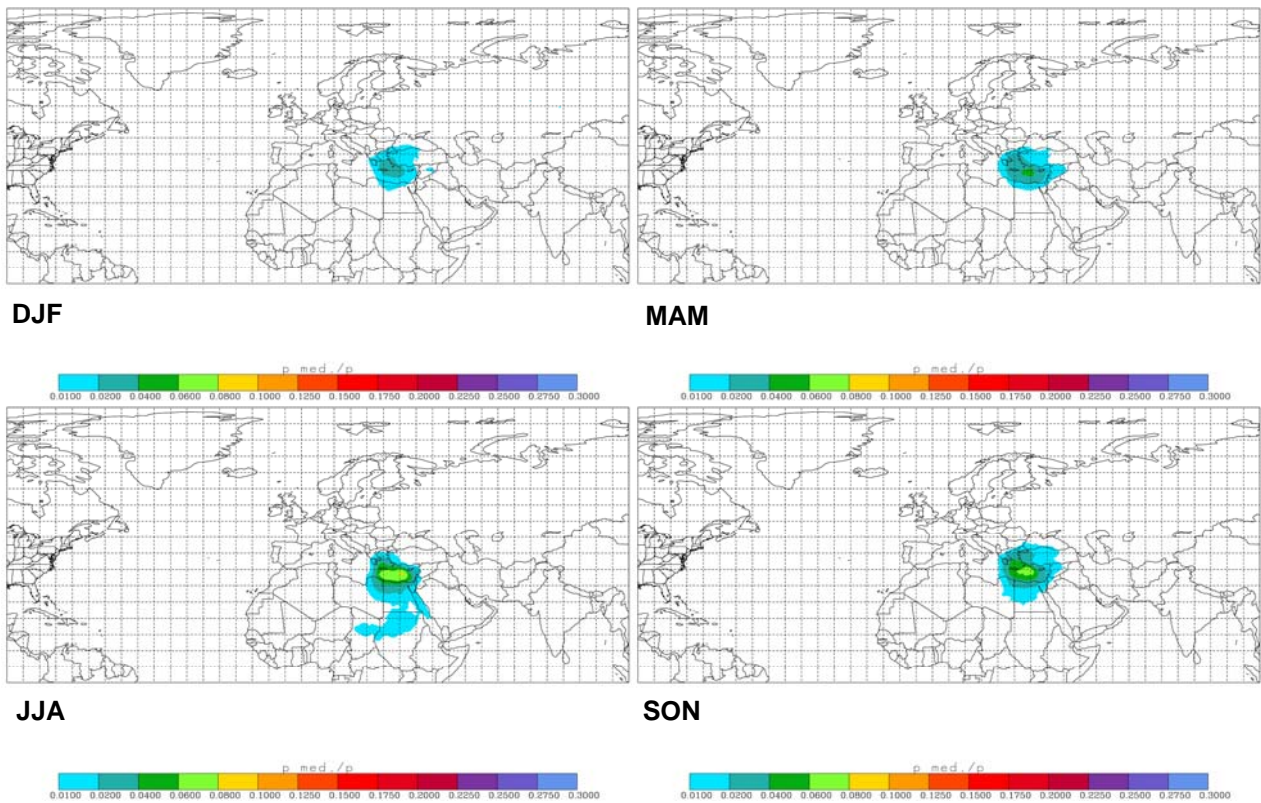


Figure 19: Same as Figure 14: but for the Etesian basin.

## Cyprus

The pattern for the easternmost sub-basin (Figure 20:) show not much difference to the moisture results, although with larger precipitation influence towards Afrika.

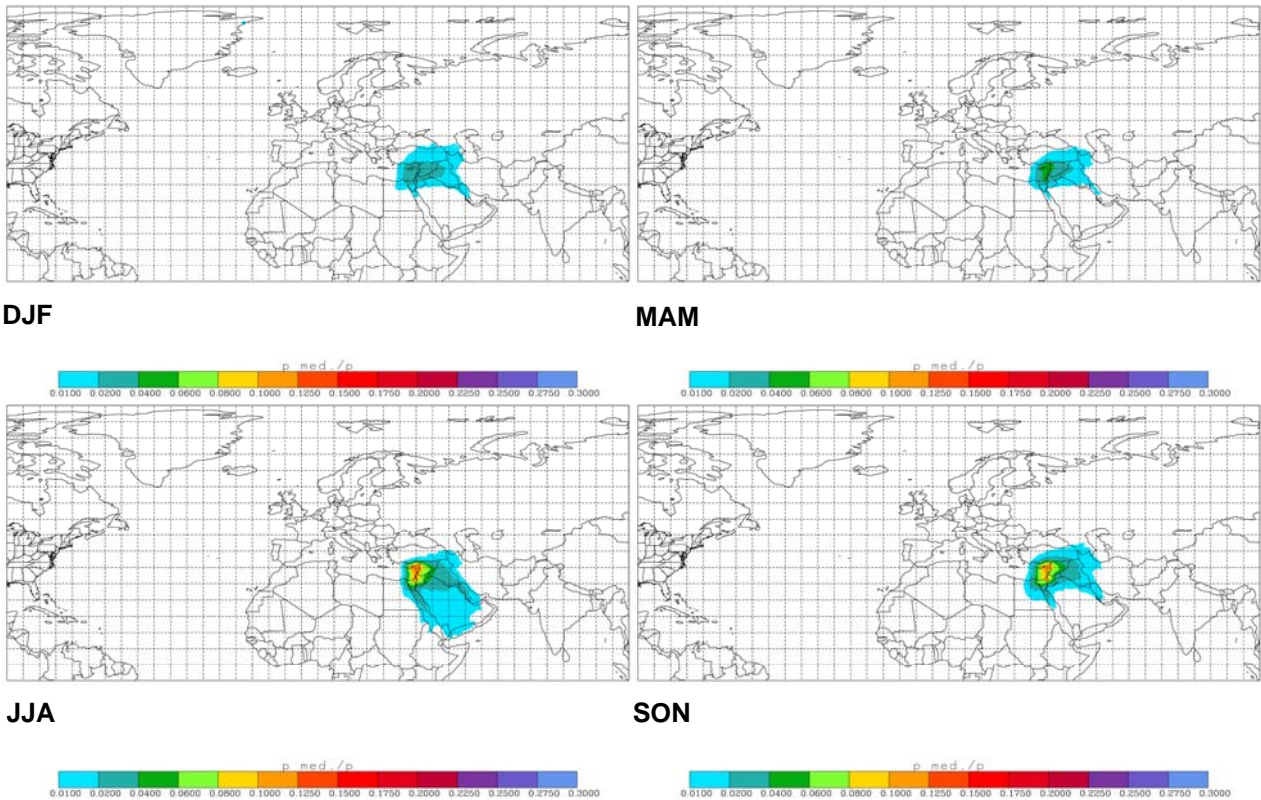


Figure 20: Same as Figure 14: but for the Cyprus basin.

---

## 6. Residence Times, Recirculation and Stagnation

### 6.1. Residence times

Residence times for particles having resided in our ROIs within a certain time window have been calculated in forward and backward mode. The residence time is defined as the average time that all tagged particles have spent in the respective evaluation grid cell if they were in the ROI during the defined time window. Residence times have been evaluated on a grid for the Mediterranean and the sub-basins for three different vertical layers:

- 0 – 1000 m agl.
- whole troposphere
- whole atmosphere (results not shown)

and different transport times interval  $\Delta t$ :

- 0 – 1 days
- 0 – 5 days
- 0 – 30 days
- 0 – 90 days

We show only residence times on an annual basis. The residence time is normalised with the number of particles in the ROI and  $\Delta t$  in days. Units are seconds per particle, receptor day, and grid cell. However, as grid cells are defined in a latitude-longitude grid, these values have been corrected to standard grid cell size (as at the equator). The grid cells for the analysis are  $1^\circ \times 1^\circ$  large. The forward mode shows the fate of Mediterranean air, while the backward mode shows where the air in the Mediterranean region came from. Particles are tagged in the forward mode if they resided initially in the ROI, in the backward mode if they arrived finally in the ROI. “Initially” and “finally” means within time intervals  $\Delta t$ , as defined above.

High residence times indicate, on one hand, areas with stagnation, and on the other hand, transport pathways. Thus they are especially relevant for air pollution budgets.

#### 6.1.1. 1-day transport time

Maxima of the 1-day residence times are of course to be expected in the middle of the ROI. In addition, high 1-day residence times reflect a tendency towards stagnation, with low wind velocities or recirculation patterns. Interestingly, the residence times are clearly higher over the Mediterranean sea areas than over adjacent land. Probably, wind velocities (mean over the ROI layer) are lower there, and maybe recirculation tendencies more pronounced. Maxima are found in the middle of the Basins, except the easternmost basin south of Cyprus. Results of forward (Figure 21:) and backward (Figure 22:) evaluations are very similar, as expected for the short transport time. The backward evaluations clearly shows that in the north, the Alps act as a barrier. The influence of the Etesians is visible in the east.

### 6.1.2. 5-day transport time

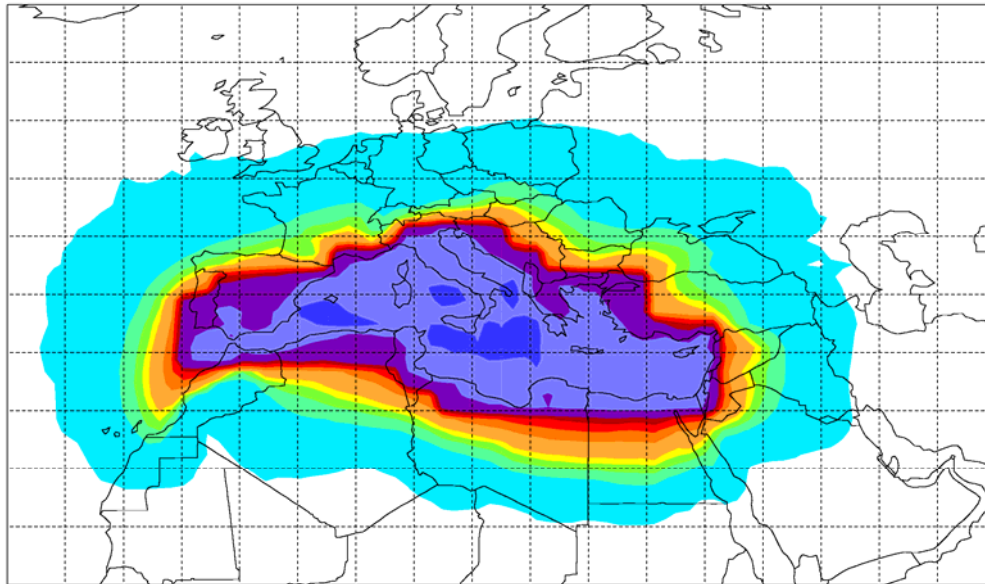
The patterns for 5-day transport times are very similar to those for one day. The maximum is found in the Tyrrhenian Sea between Southern Italy and Turkey. In the eastern Mediterranean, in the sub-region influenced by the Etesian winds, inflow from the Black Sea through the Sea of Marmara into the Aegean and outflow into the eastern part of Northern Africa is visible even in the annual means. It leads to lower residence times in the eastern part of the Mediterranean on the 5-day time scale. The overall tendency towards stagnation is still visible in the 5-day evaluations (Figure 23:, Figure 24:). In addition, the influence of the topography is clearly recognisable by minima in the atmospheric boundary layer (ABL) residence times over the mountains (the air partly flows around, and if going over the mountains has high velocities) and the channelling around them, as can be seen especially in the region of the Atlas mountains. The 5-day residence times show which influence the Mediterranean air has in northeast Europe compared to the rather small influence in northwest Europe. Influences into the Red Sea and into North Africa can also be identified as well as influences of the Ahaggar mountains and the Tibesti mountains at the southern borders of the Sahara. The influences of the mountain ridges can also be found in the 30-day and 90-day residence times.

### 6.1.3. 30-day transport time

The 30-day residence times (Figure 25:, Figure 26:) starts to illustrate the position of the Mediterranean in the global circulation which is discussed more in detail for the 90-day transport pattern. The role of mountains and sea straits becomes nicely visible both in the boundary layer and the troposphere ROI. Alps, Pyrenees, Atlas, Tibesti, Ahaggar, the Arabian and Anatolian plateau as well as the Himalayas and the Tibetan Plateau are clearly visible as regions of minima of the residence time. This is because the air flows have a tendency to go around them, and if they go over them, the wind velocities will also be higher. On the other hand, enhanced outflow through the Strait of Gibraltar and the Red Sea can be recognised. Another outflow route is over Mesopotamia, a low land between the high lands of Iran and Arabia. The Dardanelle are both an inflow and outflow route (depending on season). The longer residence times over the Western and Central Mediterranean distinguish these regions from the Eastern part.

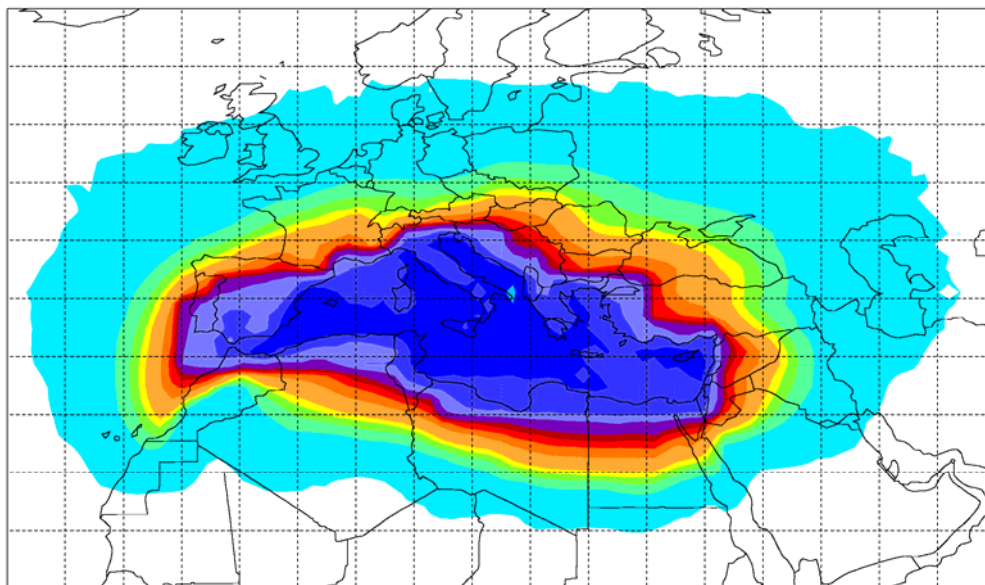
### 6.1.4. 90-day transport time

The evaluation of the residence times for 90-days (Figure 27:, Figure 28:) shows very clearly the role of the Mediterranean in the global circulation, and confirms that it can be called a crossroad of air streams (Lelieveld et al., 2002). As a broad picture, the air enters the Mediterranean mainly from the Northwest, with 90-day tropospheric source area consisting of Central and Western Europe and the North Atlantic. In general, high latitudes including arctic regions contribute. On the other hand, the outflow is split into two big flows with opposite direction. One follows the Silk Road through Central Asia north of the Tibetan Plateau to the Pacific coast. The other one leads over Northern Africa into the tropical Atlantic towards South America and the Caribbean ("Columbus' path"?) Arctic latitudes are very little influenced on this time scale.



**0 - 1000 m aql**

s / day

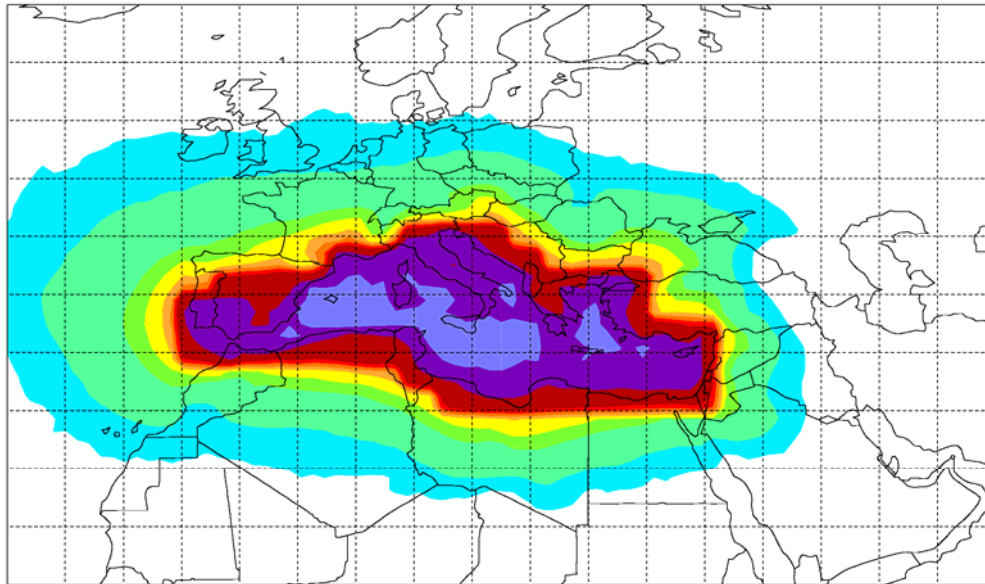


**troposphere**

s / day

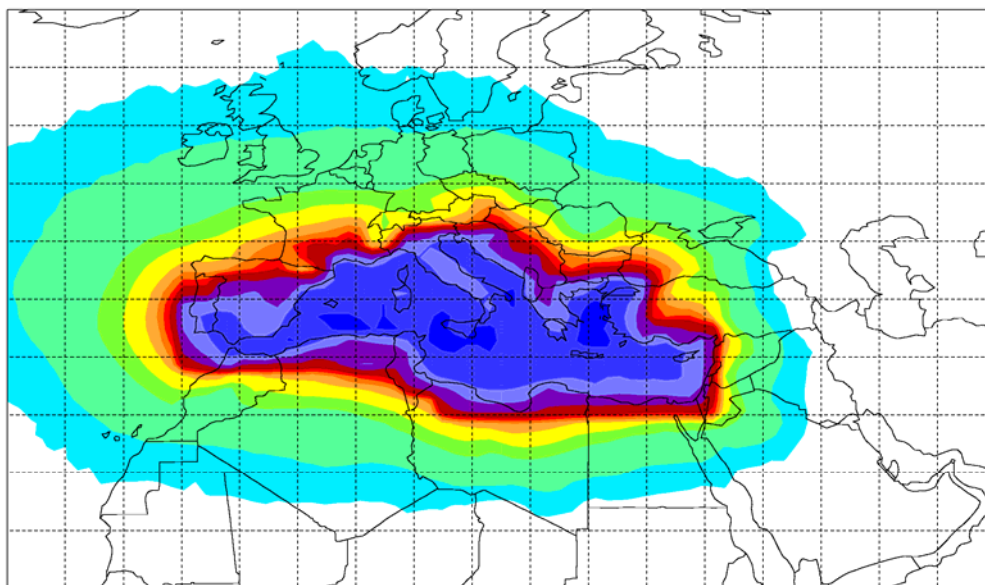
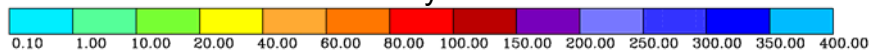


Figure 21: Residence times for 1-day transport in forward mode of the Mediterranean basin for the vertical layer 0 – 1000 agl (top) and the whole troposphere (bottom).



**0 - 1000 m**

s / day



**troposphere**

s / day

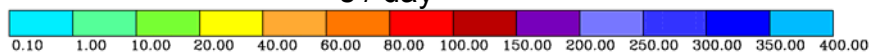
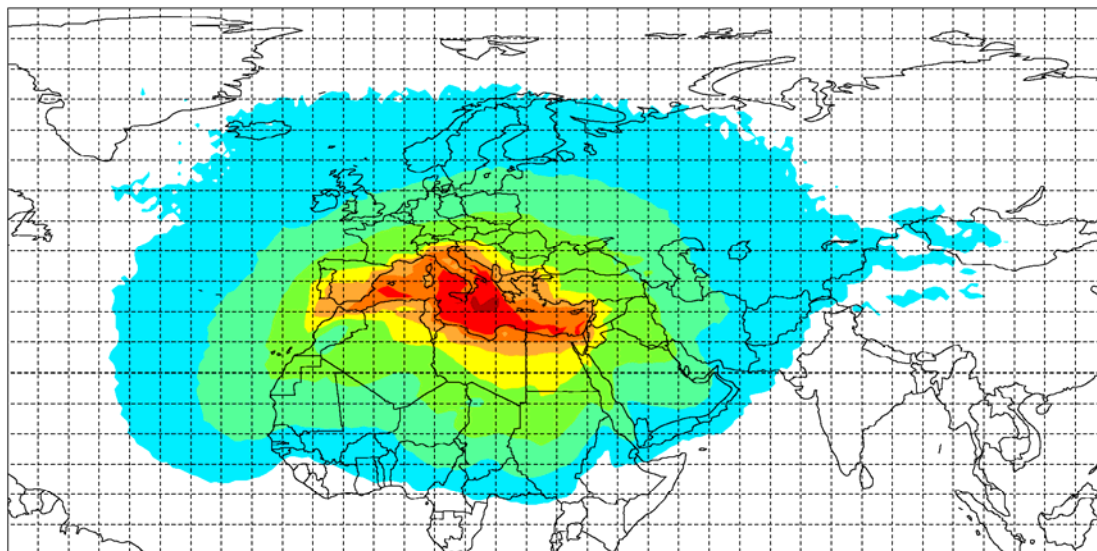
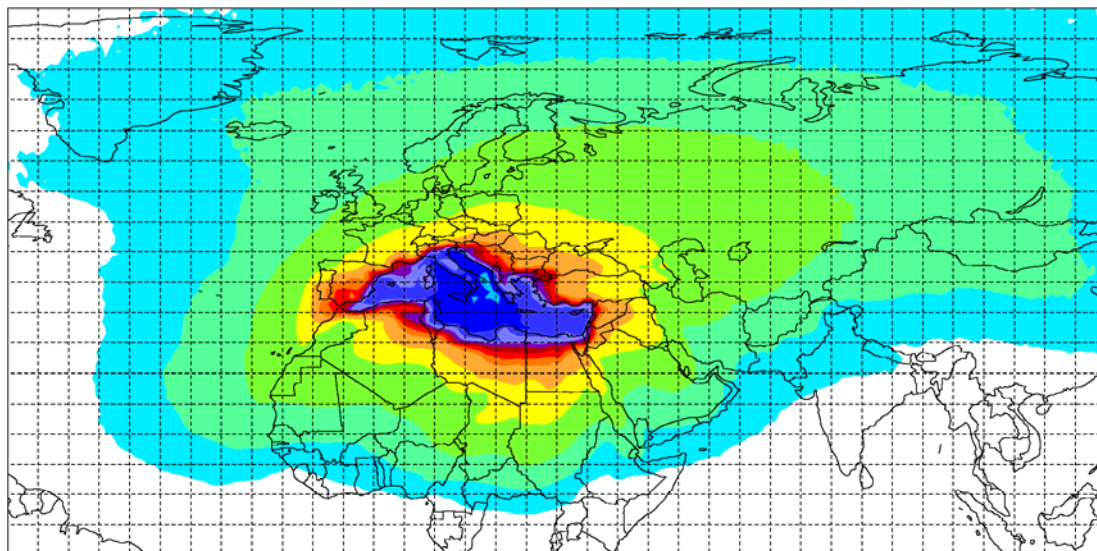
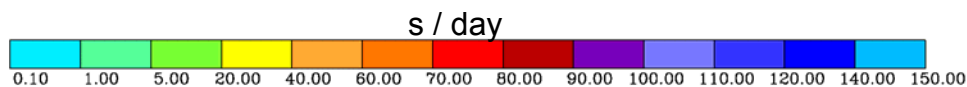


Figure 22: Residence times for 1-day transport in backward mode of the Mediterranean basin for the vertical layer 0 – 1000 agl (top) and the whole troposphere (bottom).



**0 - 1000 m agl**



**troposphere**

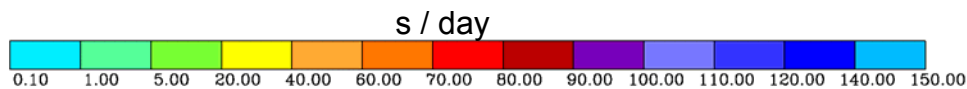
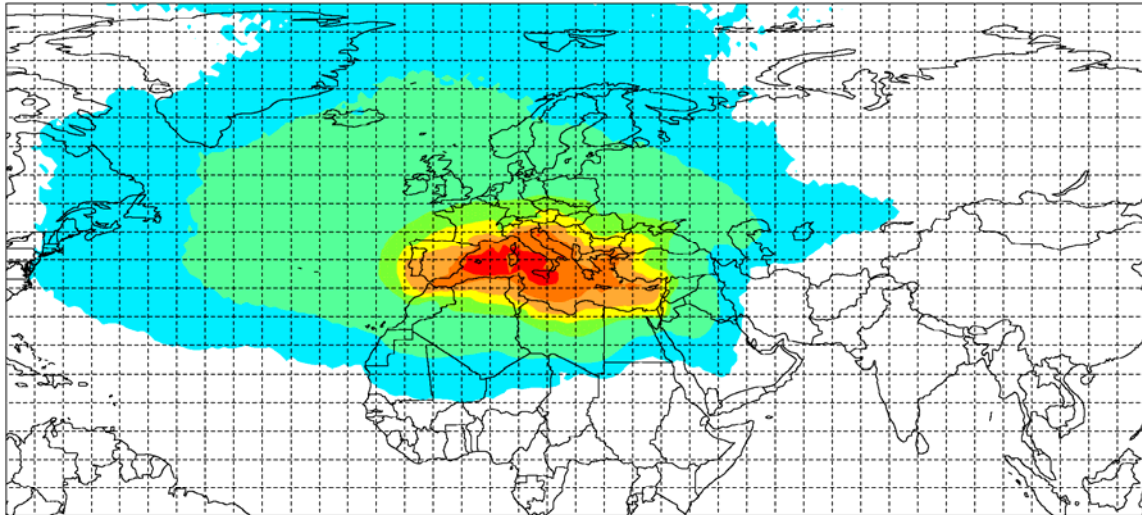
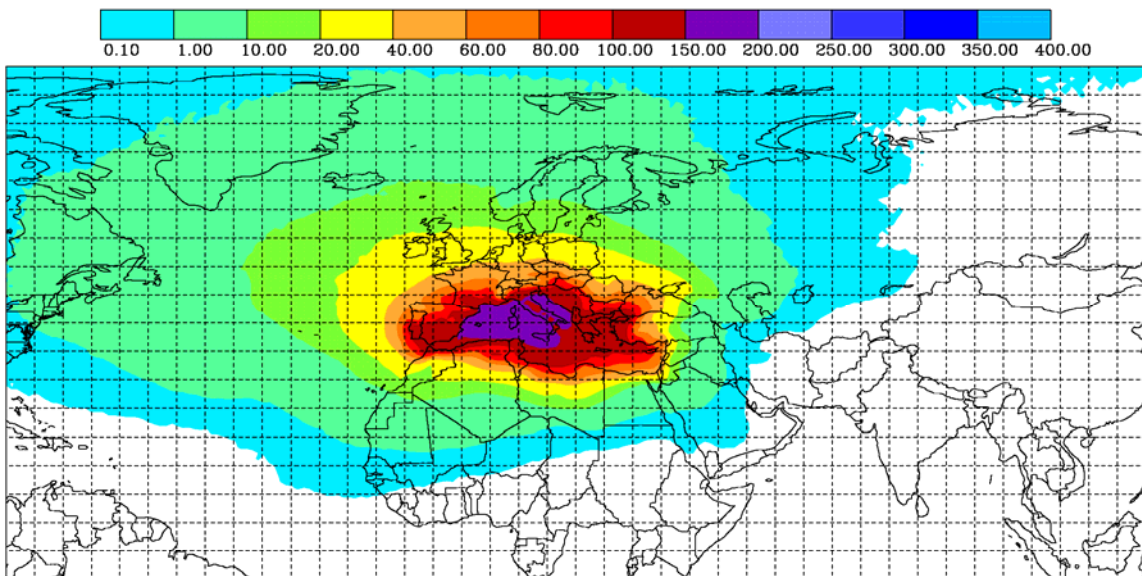


Figure 23: Residence times for 5-day transport in forward mode of the Mediterranean basin for the vertical layer 0 – 1000 agl (top) and the whole troposphere (bottom).



**0 - 1000 m agl**



**troposphere**

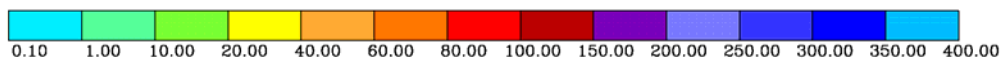
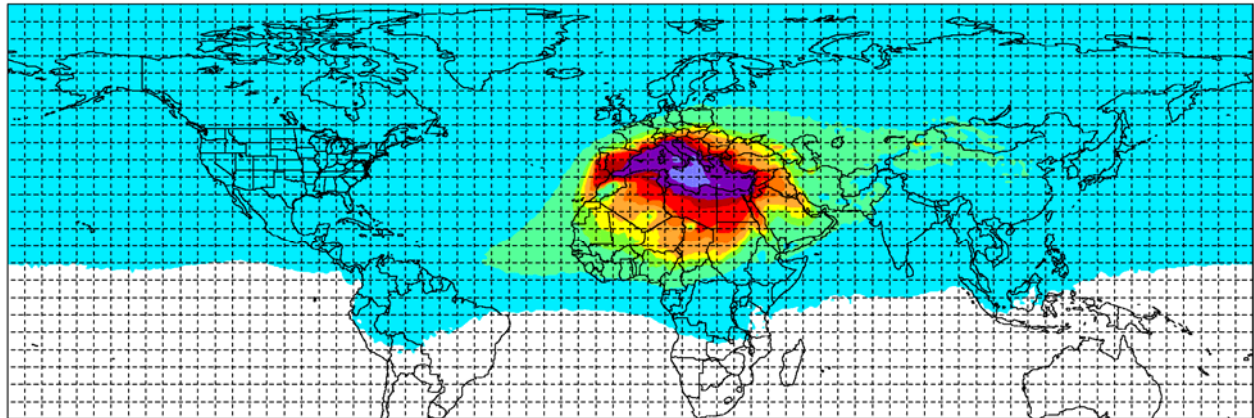
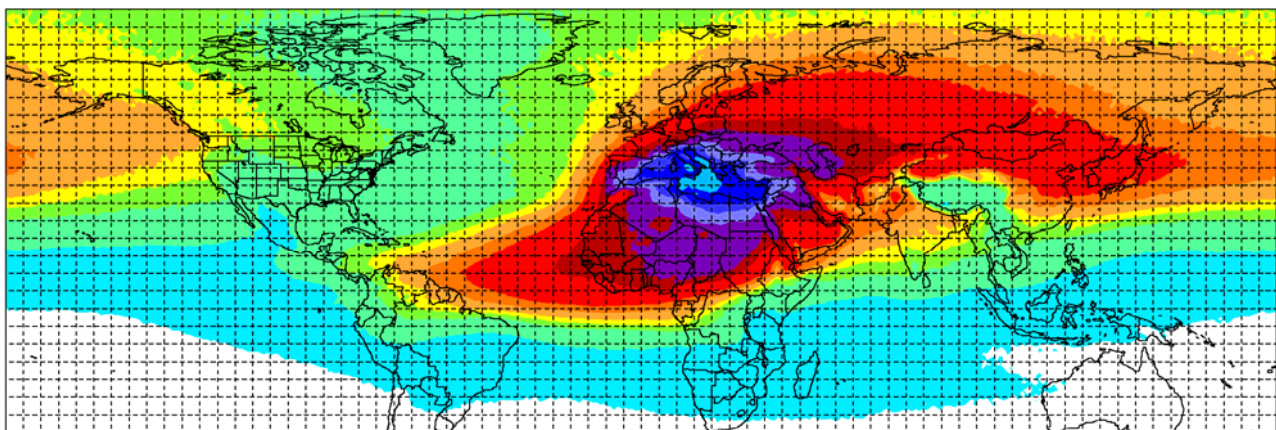
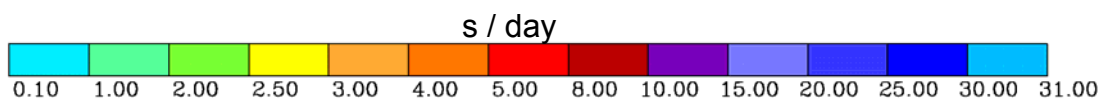


Figure 24: Residence times for 5-day transport in backward mode of the Mediterranean basin for the vertical layer 0 – 1000 agl (top) and the whole troposphere (bottom).



**0 - 1000 m agl**



**troposphere**

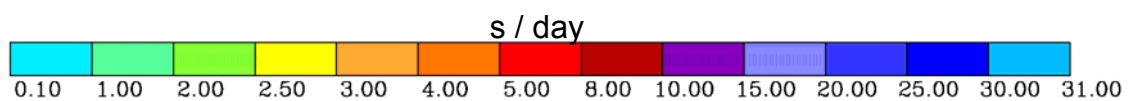
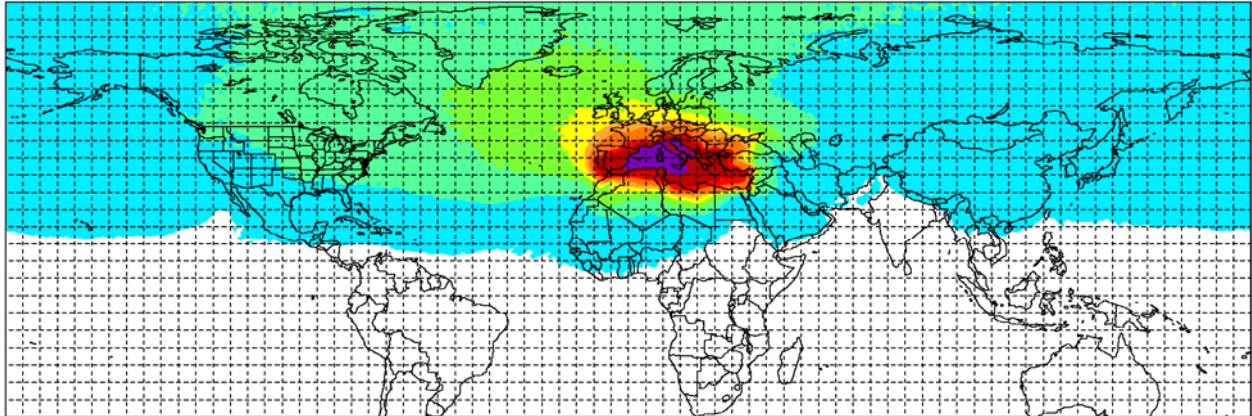
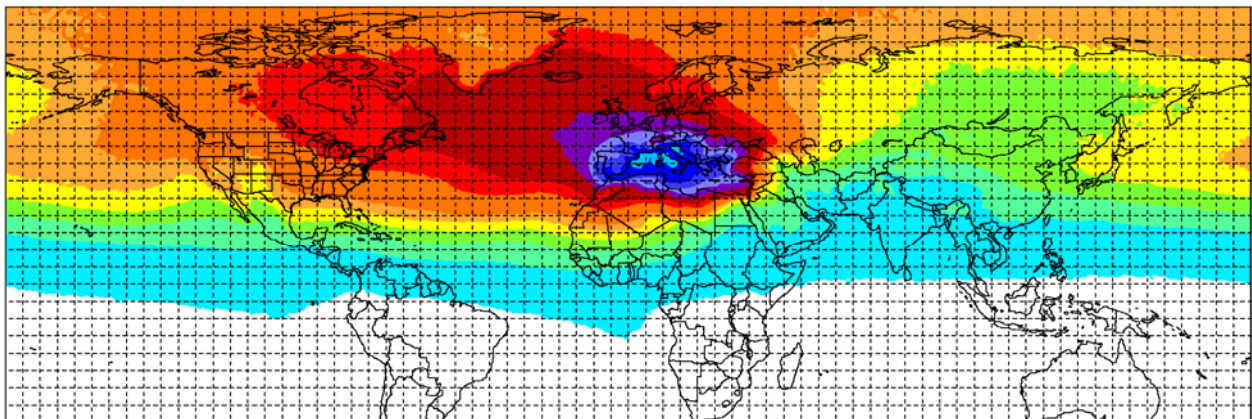
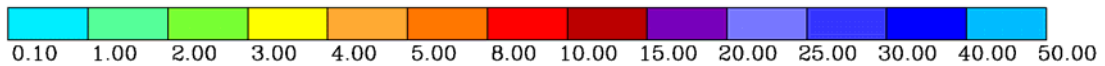


Figure 25: Same as Figure 21: but for 30-day transport times.



**0 - 1000 m**

s / day



**troposphere**

s / day

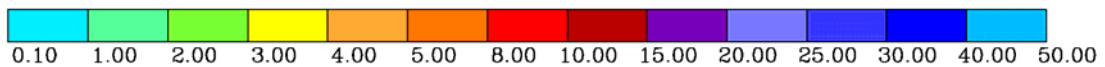
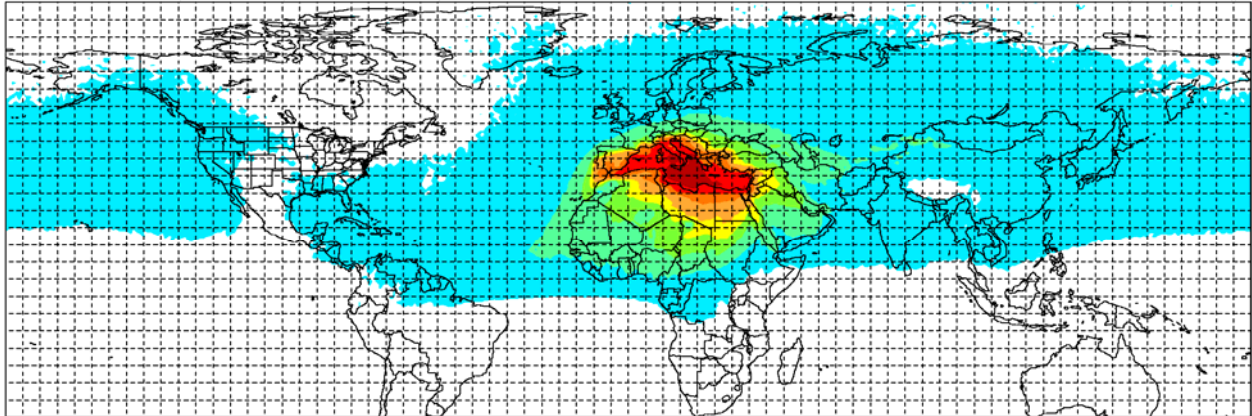
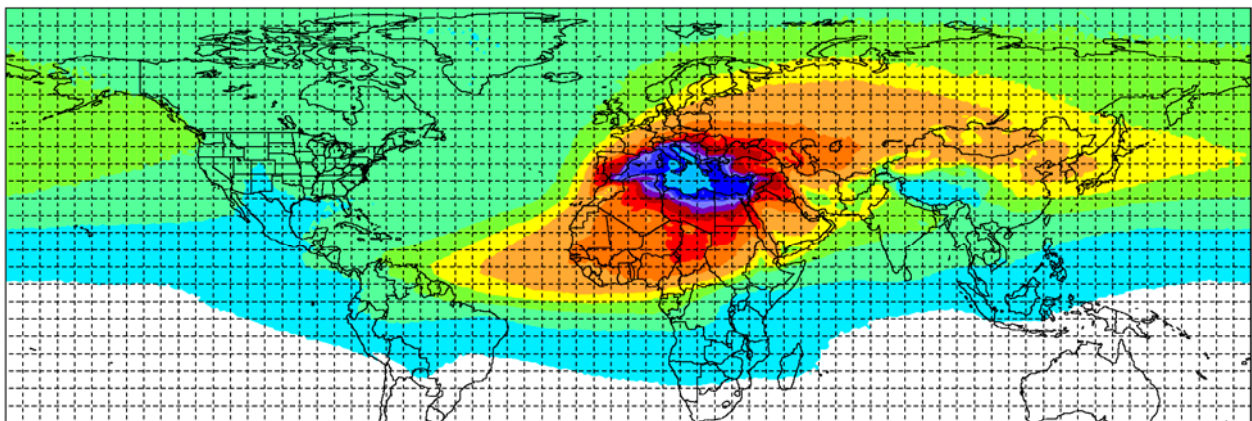
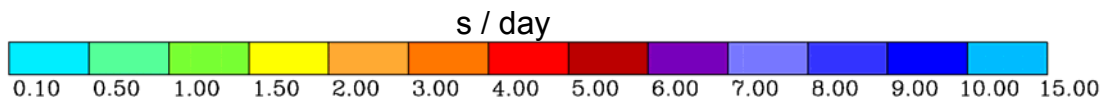


Figure 26: Same as Figure 22: but for 30-day transport times.



**0 - 1000 m**



**troposphere**

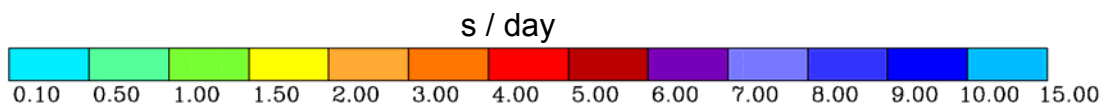
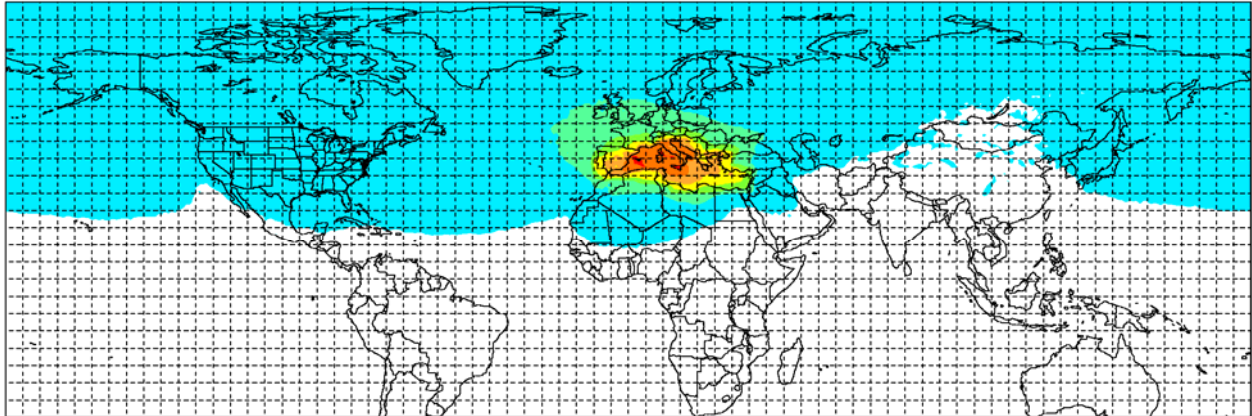
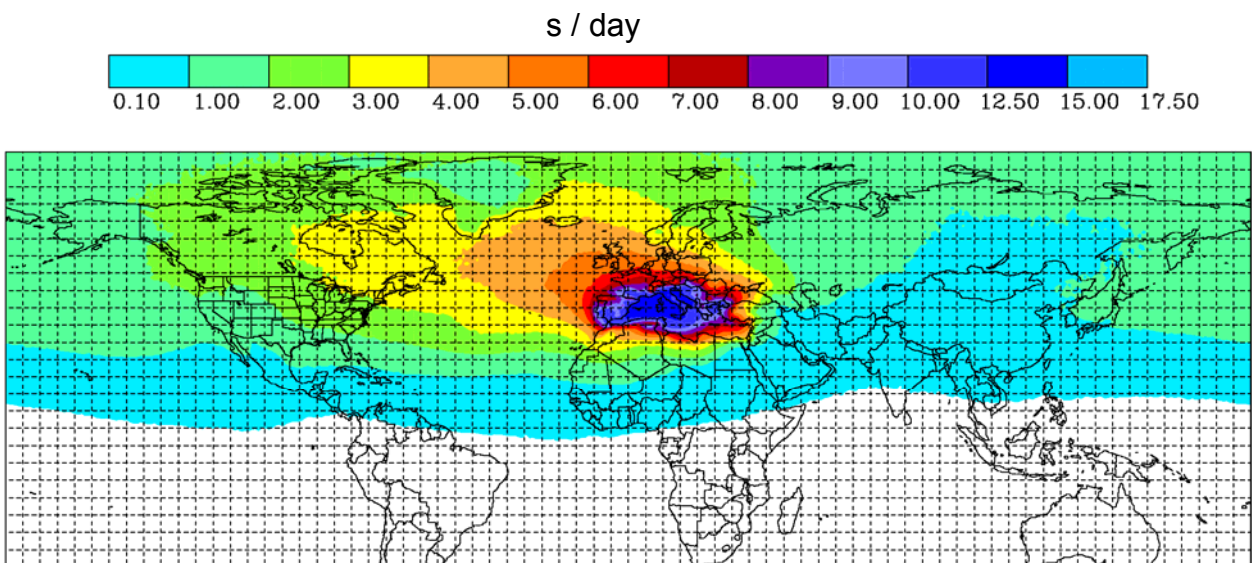


Figure 27: Same as Figure 21: but for 90-day transport times.



## 0 - 1000 m



## troposphere

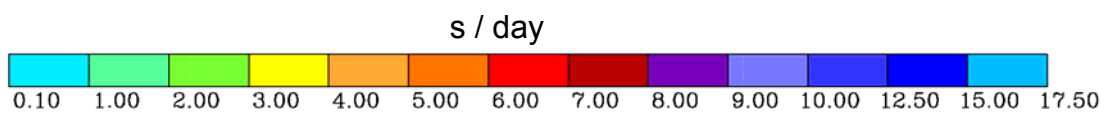


Figure 28: Same as Figure 22: but for 90-day transport times.

## 6.2. Stagnation and Recirculation

The residence times already give an idea of regions where the air stays a long time, and especially residence times with short time intervals are related to stagnant conditions. To show such areas more clearly, additional analyses for stagnation and recirculation have been carried out (see Allwine and Whiteman, 1994, for background to these terms). Stagnation is defined as the vectorial mean of the particle velocities, or in short, the distance between start point and end point of a particle divided by the length of the time interval. These values are averaged over all the particles in a grid cell and are presented in units of kilometre per day (low value means strong stagnation). Recirculation means that the air is moving, but after some time returning to near its origin. The intensity of recirculation is calculated as the ratio between vectorial and scalar means of the displacement vectors and thus lies between 0 (total recirculation) and 1 (totally straight movement).

Recirculation and stagnation have been calculated for the four seasons and for the whole world for different time intervals  $\Delta t$ . These time intervals are shorter than time intervals used for the residence times, namely for 1 day, 3 days (recirculation only) and 5 days. As they are local data, not relationships between a source or a receptor region and the rest of the world, it is not necessary to do separate ROI calculations. We present here results for the Mediterranean region only.

### 6.2.1. Stagnation

1-day stagnation, Figure 29:, shows that in winter a dominant streak with strong transport enters the Mediterranean at the gulf of Lyon, a consequence of large-scale channelling between the Alps and the Pyrenees. Interestingly, it continues through the strait between Tunisia and Sicily and then in weaker form passes south of Crete and reaches even the eastern end of the Mediterranean basin. In summer, the dominant region with low stagnation (i.e., strong displacements) is the Etesian region in the Aegean Sea. We see that this flow continues over the whole Mediterranean basin into North Africa. Autumn and spring are a mixture of these two patterns, with much more stagnation over North Africa in autumn than in spring.

Areas of stagnation are the Po Basin, known to be an area with high air pollution, the Gulf of Venice, the Atlas mountains, the Sicilian Sea and Turkey. In spring and autumn the regions of stagnation are distributed very similar with low transportation in the Balearic Sea and Adriatic Sea.

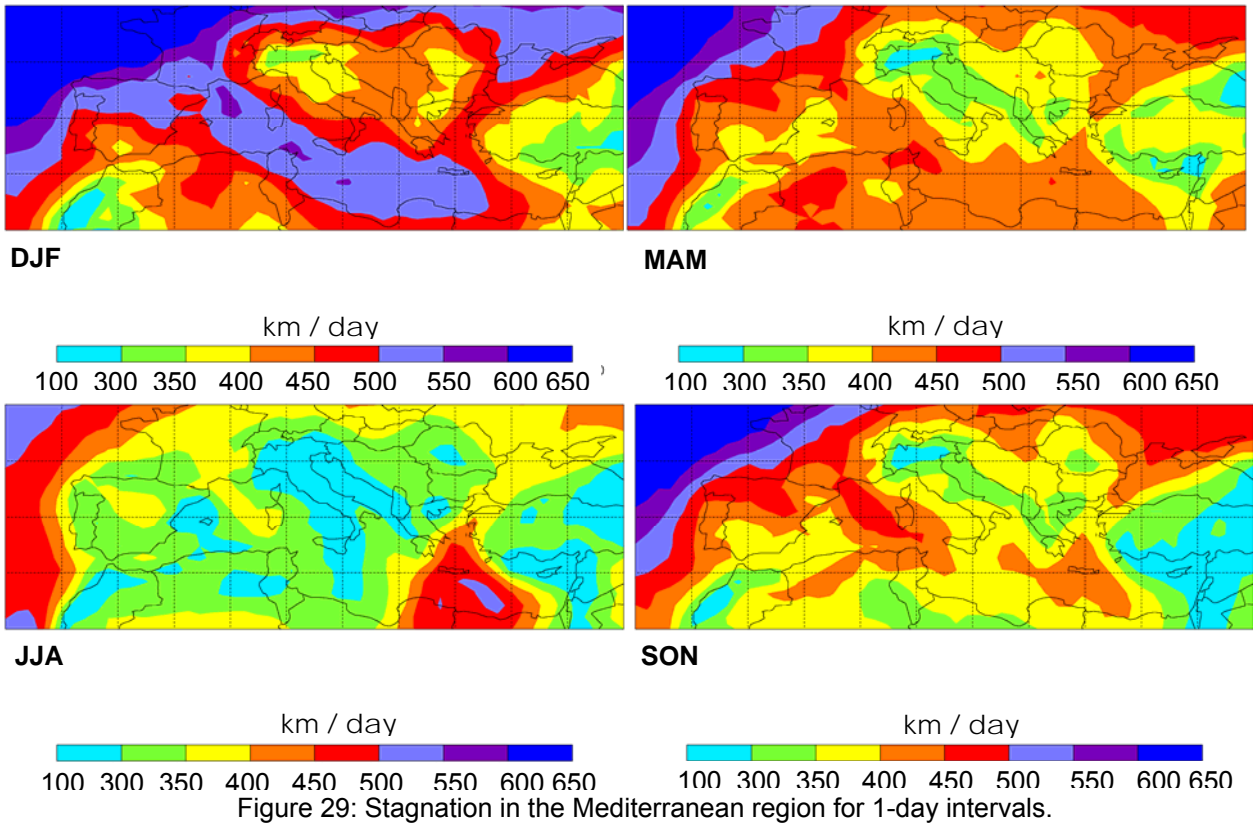
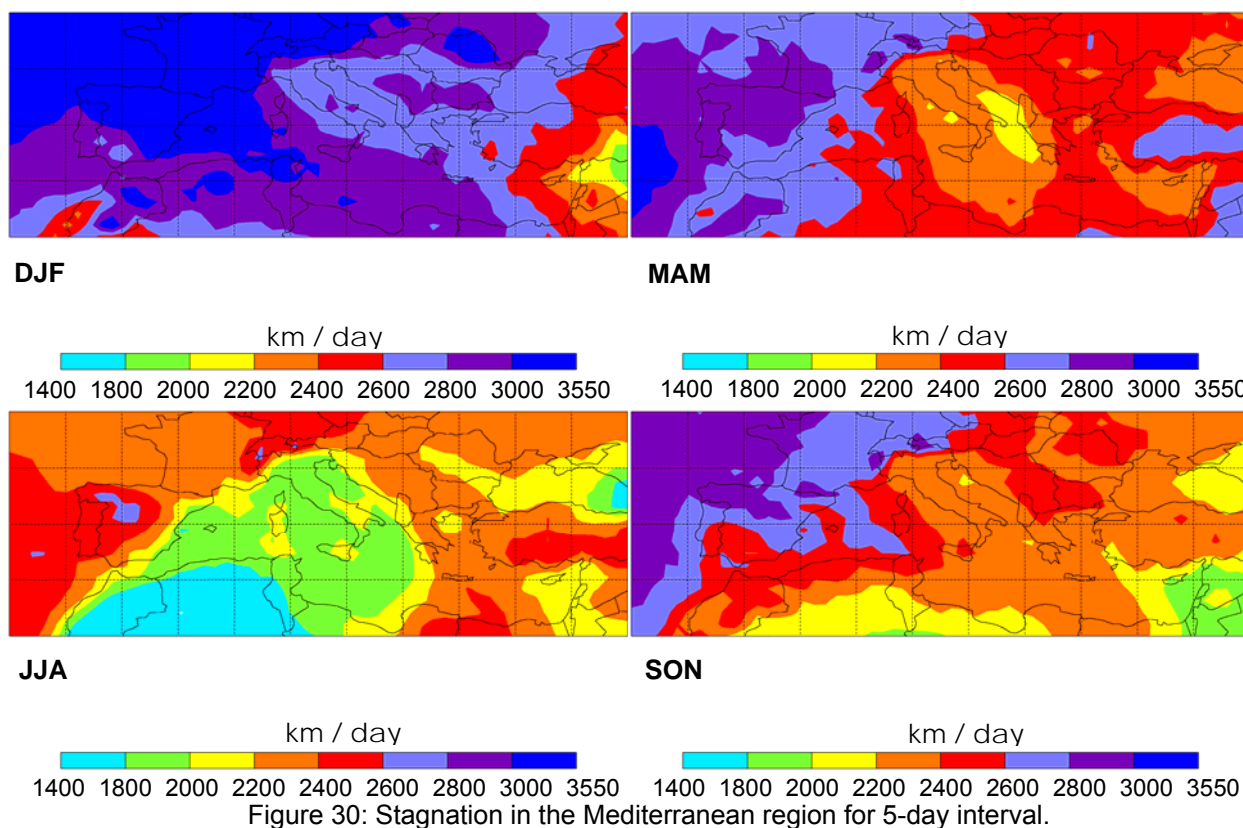


Figure 29: Stagnation in the Mediterranean region for 1-day intervals.

5-day stagnation results, Figure 30:, show that the region with highest stagnation in summer is the western Mediterranean basin and the region around Cyprus, which is also present in the other three seasons.



### 6.2.2. Recirculation

As explained above, recirculation is presented here as fraction between 0 and 1 where 0 means total recirculation. On the average over a whole season, these values vary only between 0.45 and 0.56 for the 1-day interval that would be sensitive to thermal circulations, as these have a 1-day period. This indicates that on the scale of this analysis such circulations are not a dominant feature.

In the results of  $\Delta t = 1$  day (Figure 31:) the mountainous areas surrounding the Mediterranean are clear identifiable as regions with high values (low recirculation) for all seasons. Although diurnal wind systems involving some degree of recirculation are known to be present in mountain regions, they do not show up in this analysis because their scale (e.g. inside valleys) is not resolved by the ECWMF input data. Instead, over the mountains synoptic winds are stronger and more dominant and this is the cause of this result. Recirculation would be expected to be most pronounced in

summer, and indeed lowest values (more recirculation) are found in this season, mainly over sea, including the western Mediterranean between Sardinia and Spain, the southern Adriatic Sea, and the Aegean. In the other seasons, these regions are also present as recirculation maxima. However, the sea between Algeria and Spain, including the area between the Balearic Islands and the Spanish continent is not part of the minimum region. It comes as a surprise that areas with dominant advective flow patterns such as the Etesian region (or at least a part of it) and the Gulf of Lyon are areas of low values (higher recirculation tendency) in all seasons. At the moment we have no real explanation for this feature, except that maybe there is some synoptic variability in these flows leading to such a result.

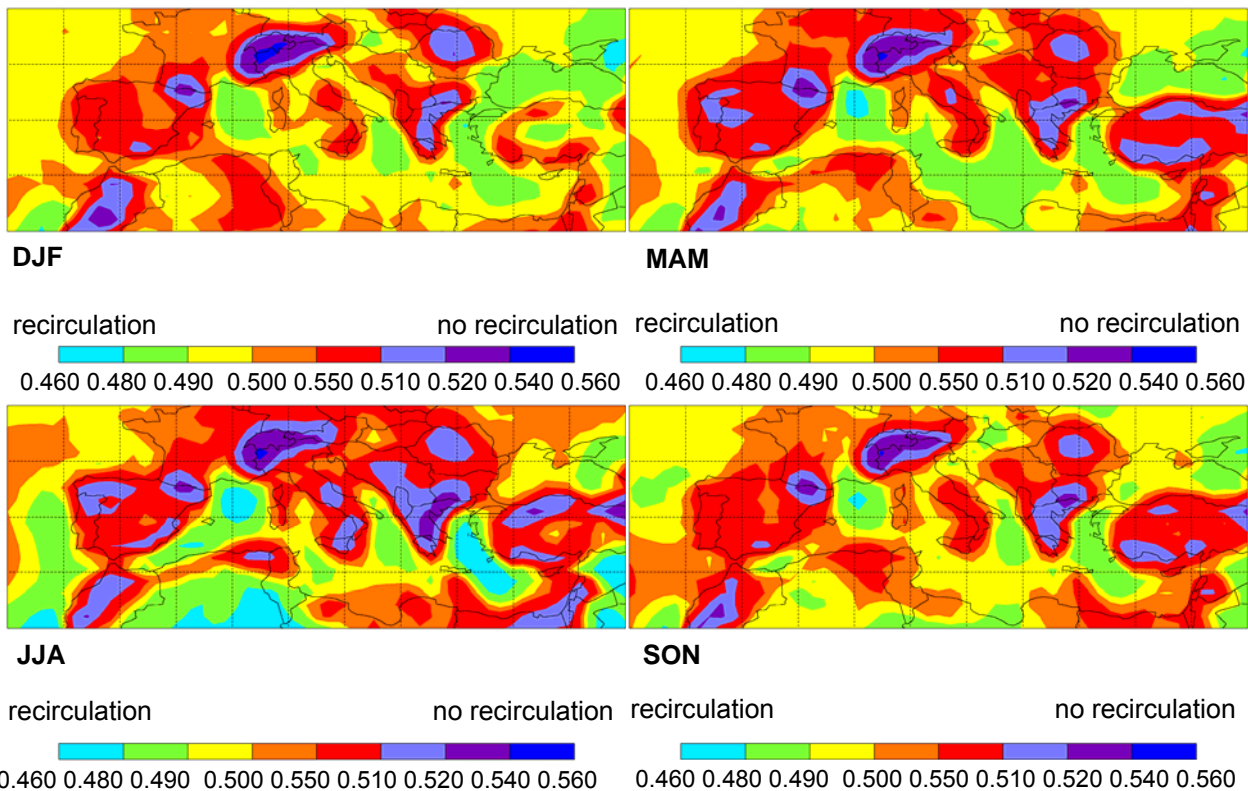
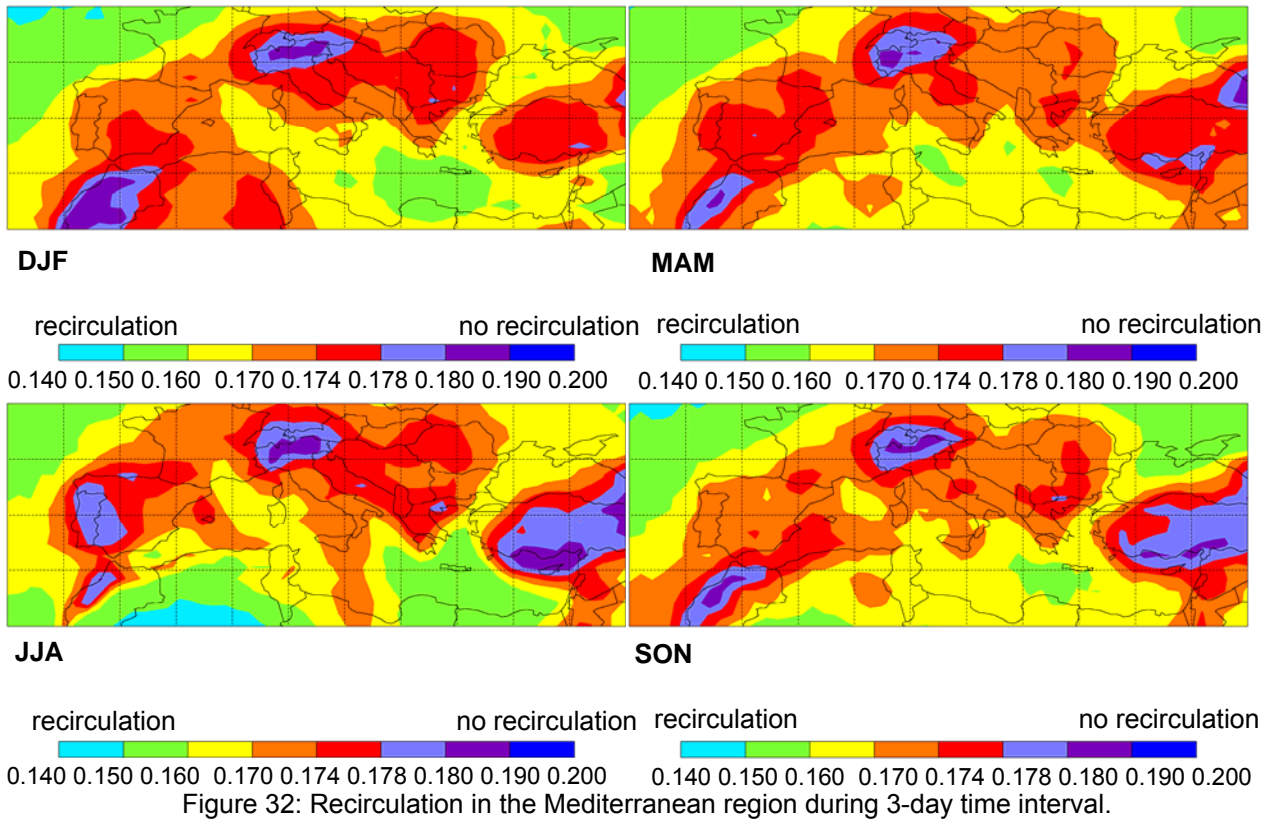
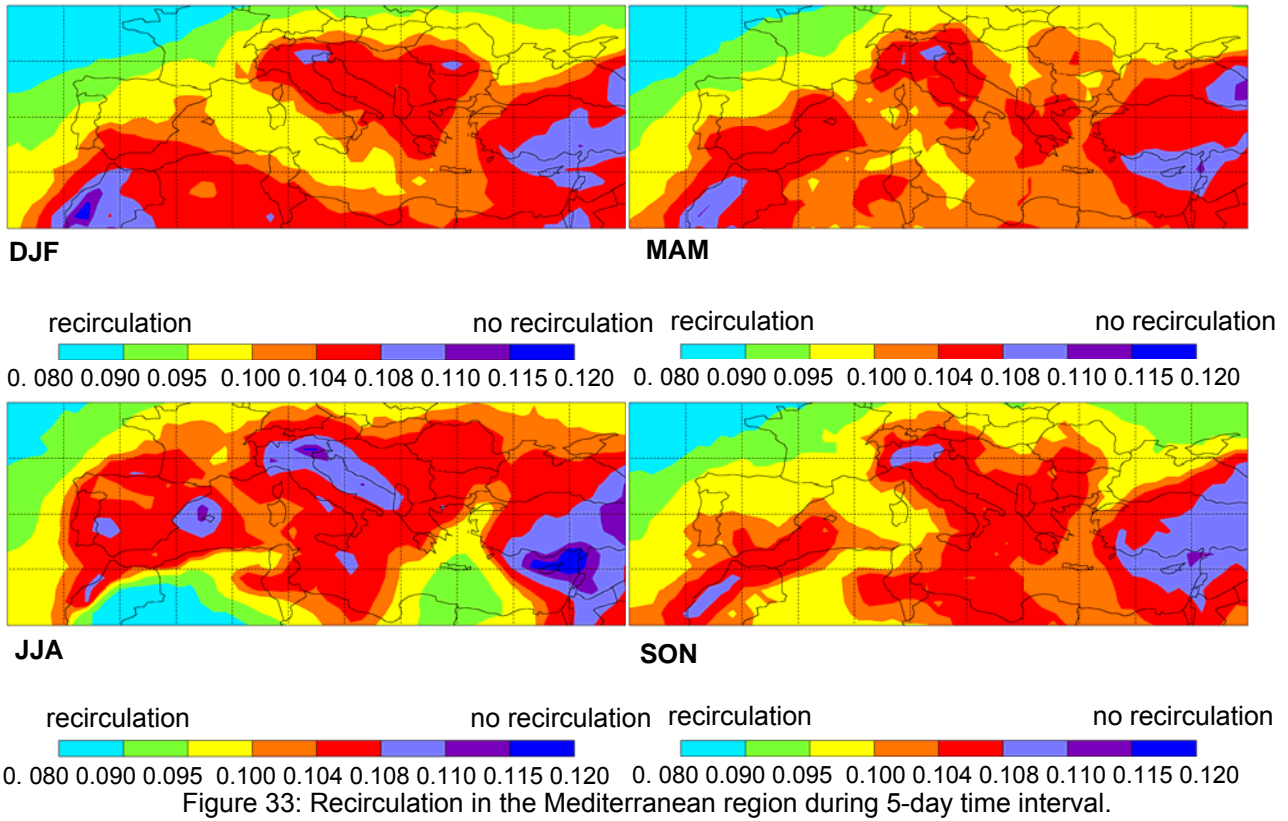


Figure 31: Recirculation in the Mediterranean region during 1-day time interval.

3-day (Figure 32:) and 5-day recirculation ratios (Figure 33:) are more influenced by synoptic features such as cyclones and exhibit considerably lower values than the 1-day values. Also the different Mediterranean basins do not show up as separate regions. Ratios are in general higher inside the Mediterranean than outside to the north and west, probably indicating less cyclonic activity in the Mediterranean. This is most striking for the 5-day period in summer. The region affected by the Etesian winds is a low-value region (more recirculation) also on this longer time scale, again a kind of surprise.





## 7. Conclusions

Evaluations of the fate and origin of Mediterranean air and atmospheric moisture were carried out based on a Lagrangian transport data set generated with 1° operational ECMWF data and the Lagrangian particle dispersion model FLEXPART (Stohl et al., 2005). The period 27 October 1999 - 1 May 2005 has been investigated. It contains on one hand two extreme events, the heavy Central European flooding event in 2002, and a drought event in 2003. On the other hand it has no extremes of climate modes such as ENSO or NAO, which also influence the conditions in the Mediterranean area. The coarse resolution of the data set is not suitable to make single-year or even one-season analyses, therefore only averages over the full period were analysed.

Residence time analyses, especially of the 30 d and 90 d residence times, show that the Mediterranean is a crossroad of air streams (Fig. 5) where the air arrives mainly from the northwest and then is split into two major branches. The first one continues eastwards through Central Asia. The second one bends southwards into North Africa and continues towards southwest over the tropical Atlantic following the trade winds. The source regions for the Mediterranean indicate that the high-latitude regions over the North Atlantic and Canada contribute, while the outflow does not enter any high latitude regions within 90 days. This confirms climatologically the conclusions drawn by Lelieveld et al. (2002) who found similar pathways in summer during their MINOS campaign in 2001.

Another interesting feature is the channeling by mountains and sea straits which is best visible in the 5 d and 30 d residence times with minima over the mountains and maxima along the straits, e.g. the strait of Gibraltar, the Red Sea and the Dardanelles as outflow routes. Another channelled outflow route is over Mesopotamia, a lowland between the highlands of Iran and Arabia. The preferred inflow channel is the Gulf of Lyon between the Pyrenees and the Alps. Longer residence times are found over the Western and Central Mediterranean than over the Eastern Mediterranean which is strongly influenced by the Etesian wind crossing the basin.

Stagnation results show a strong seasonal dependency. In winter and spring, the Po Basin, the Adriatic Sea and the region between Turkey and Cyprus show the strongest stagnation. In summer, also the Balearic region and the surroundings of the Italian peninsula have a tendency towards increased stagnation.

Results of the moisture and precipitation analyses show that the Mediterranean basin contributes to the whole northern hemisphere, although with a low fraction. Highest fraction of atmospheric moisture and precipitation are located above the Mediterranean Sea itself with a maximum up to 11 % in summer. Sub-basin analyses show that the Western Mediterranean basin has its main influence on the European continent and the Alpine region, a conclusion also drawn by Sodemann and Zubler (2010). Influences of the eastern Mediterranean basin are mainly in the area of the Middle East and northern Africa. On a smaller scale, as for the Adriatic basin or the Balearic basin, contributions are mainly locally: the Adriatic basin shows its relevance for the Balkan countries, Austria and the Po basin in northern Italy; the Balearic basin shows a significant contribution of up to 5% of the Mediterranean moisture fraction on the adjacent portion of Spain. An increase of the precipitation fraction can be found in autumn when higher SSTs influence the evaporation from the ocean reaching its maximum in November and December (Mariotti et al., 2002).

Mediterranean moisture flux evaluations confirm all the previously mentioned air pathways and crossing the Mediterranean basin. Besides the three already mentioned airstreams, some additional streams are present. In summer and autumn, three ingestions paths with up to  $60 \text{ kg}(\text{ms})^{-1}$ , into the Intertropical Convergence Zone over Egypt, Libya, and Tunisia are identified, respectively, while in the other seasons the path over Egypt dominates. The influence of the westerlies is present in all seasons, although smaller in summer. Local wind systems, such as the Etesians in summer or the Sirocco in autumn, winter, and spring are especially present in the lowest 1000 m. Another pathway goes into the Mesopotamia, showing with up to  $125 \text{ kg}(\text{m s})^{-1}$  the relevance of the Mediterranean basin for this area.

Higher resolved input data as with the new ECMWF resolution plus more particles released would be useful to investigate especially small scale features more deeply. Evaluations of a longer time period would also be useful for a more detailed analysis, especially when analysing in a climatological sense.

Of course, there are many possibilities for interesting future work, though with the resources given they are probably out of the scope of our Circe contribution. Here we just present a few topics:

- Clarification of the results for recirculation. Investigation of stagnation and recirculation in terms of fraction of the time when a threshold of these parameters is exceeded rather than the means over a season.
- Combination of residence times with data bases of air pollution emissions to create also budgets of air pollution.
- New Lagrangian transport calculations for recent periods with  $0.2^\circ$  ECMWF data, a better resolved output grid and more particles, but on a limited domain, to study better smaller scale circulations. As a first step, it would be useful to check these ECMWF data with respect to their ability of reproducing land-sea wind patterns in the Mediterranean.

## 8. References

- Allwine K.J., Whiteman C.D., 1994: Single-station integral measures of atmospheric stagnation, recirculation and ventilation. *Atmos. Environ.*, 28, 713-721.
- Anker, Y., Flexer, A., Rosenthal, E., and Ganor, E. , 2007: Relationship between the origin of precipitation in the Jordan Rift valley and their geochemical composition, *J. Geophys. Res.*, 112, D03306, doi:10.1029/2006JD007517.
- Drumond, A., R. Nieto, L. Gimeno, and T. Ambrizzi (2008), A Lagrangian identification of major sources of moisture over Central Brazil and La Plata Basin, *J. Geophys. Res.*, 113, D14128, doi:10.1029/2007JD009547.
- Gallego, D, Jimenez, J. M. , Ribera, P., and V. Cifuentes (2008) Computing moisture sources in small river basins by lagrangian methods: the example of the Guadalquivir river (Southern Spain), *Geophysical Research Abstracts*, Vol. 10, EGU2008-A-02505, 2008, SRef-ID: 1607-7962/gra/EGU2008-A-02505, EGU General Assembly 2008
- James, P., A. Stohl, N. Spichtinger, S. Eckhardt, and C. Forster. (2004) Climatological aspects of the extreme European rainfall of August 2002 and a trajectory method for estimating the associated evaporative source regions. *NHESS* 4, 733–746.
- J. Lelieveld, H. Berresheim, S. Borrmann, P. J. Crutzen, F. J. Dentener, H. Fischer, J. Feichter, P. J. Flatau, J. Heland, R. Holzinger, R. Korrman, M. G. Lawrence, Z. Levin, K. M. Markowicz, N. Mihalopoulos, A. Minikin, V. Ramanathan, M. de Reus, G. J. Roelofs, H. A. Scheeren, J. Sciare, H. Schlager, M. Schultz, P. Siegmund, B. Steil, E. G. Stephanou, P. Stier, M. Traub, C. Warneke, J. Williams, and H. Ziereis (2002): Global Air Pollution Crossroads over the Mediterranean. *Science* **298** (5594), 794-799. [DOI: 10.1126/science.1075457]
- Mariotti, A., Struglia, M.V., Zeng, N., and K.-M. Lau (2002) The hydrological cycle in the Mediterranean region and implications for the water budget of the Mediterranean Sea., *Journal of Climate*, Vol 15, No 13, pages: 1674-1690
- Nieto R., Gimeno L., Trigo R.M. (2006) A Lagrangian identification of major sources of Sahel moisture . *Geophysical Research Letters*, 33, L18707, doi:10.1029/2006GL027232.
- Nieto, R., L. Gimeno, D. Gallego, and R. Trigo (2007), Contributions to the moisture budget of airmasses over Iceland, *Meteorol. Z.*, 16, 37– 44.
- Nieto, R., Gallego, D., Trigo, R., Ribera, P. and L. Gimeno (2008a) Dynamic identification of moisture sources in the Orinoco basin in equatorial South America, *Hydrological Sciences Journal*, 53, 602-617
- Nieto, R., L. Gimeno, and R. Trigo (2008b), A Lagrangian identification of major sources of Mediterranean region moisture, 2nd HyMeX workshop, 2-4 June 2008, Ecole Polytechnique, Palaiseau, France. [http://www.cnrm.meteo.fr/hymex/ps\\_pdf\\_abstracts\\_june\\_2008/poster\\_83.pdf](http://www.cnrm.meteo.fr/hymex/ps_pdf_abstracts_june_2008/poster_83.pdf) (access 19.12.2008)

- Sodemann, H., (2006) *Tropospheric transport of water vapour: Lagrangian and Eulerian perspectives*, Diss. ETH No. 16623, Swiss Federal Institute of Technology Zurich, Logos Verlag, Berlin, 250 pp
- Sodemann, H. and Zubler, A., 2007 Herkunft des Niederschlagswassers im Alpenraum. *DACH Meteorologentagung 2007, Hamburg*.
- Sodemann, H. and Zubler, E. , 2010: Seasonality and inter-annual variability of the moisture sources for Alpine precipitation during 1995–2002, *Int. J. Climatol.*, 30, 947–961, doi:10.1002/joc.1932.
- Sodemann, H., Masson-Delmotte, V., Schwierz, C., Vinther, B. M., and Wernli, H. , 2008b: Inter-annual variability of Greenland winter precipitation sources: 2. Effects of North Atlantic Oscillation variability on stable isotopes in precipitation., *J. Geophys. Res.*, 113, D12111, doi:10.1029/2007JD009416.
- Sodemann, H., Schwierz, C., and Wernli, H. , 2008a: Inter-annual variability of Greenland winter precipitation sources: 1. Lagrangian moisture diagnostic and North Atlantic Oscillation influence., *J. Geophys. Res.*, 113, D03107, doi:10.1029/2007JD008503.
- Stohl, A., M. Hittenberger, and G. Wotawa (1998) Validation of the Lagrangian particle dispersion model FLEXPART against large scale tracer experiments. *Atmos. Environ.* 32, 4245-4264
- Stohl, A., and D. J. Thomson (1999) A density correction for Lagrangian particle dispersion models. *Bound.-Layer Met.* 90, 155-167
- Stohl, A., and P. James. (2004) A Lagrangian analysis of the atmospheric branch of the global water cycle. Part I: Method description, validation, and demonstration for the August 2002 flooding in Central Europe. *J. Hydrometeorol.* 5, 656– 678.
- Stohl, A., C. Forster, A. Frank, P. Seibert, and G. Wotawa (2005) Technical Note : The Lagrangian particle dispersion model FLEXPART version 6.2. *Atmos. Chem. Phys.* 5, 2461-2474
- Stohl, A. (2006) Characteristics of atmospheric transport into the Arctic troposphere. *J. Geophys. Res.* 111, D11306, doi:10.1029/2005JD006888.
- Wernli, H. and H. C. Davies (1997), A Lagrangian-based analysis of extratropical cyclones. I: The method and some applications, *Q. J. R. Meteorol. Soc.*, 123, 467-489
- Wernli, H. (1997), A Lagrangian-based analysis of extratropical cyclones. II: A detailed case-study, *Q. J. R. Meteorol. Soc.*, 123, 1677– 1706.1
- Zecchetto S. and F. De Biasio (2007), Sea surface winds over the Mediterranean Basin from satellite data (2000-2004): meso- and local-scale features on annual and seasonal timescales, *J. Appl. Meteorol. Climatol.* , 46 (6), 814-827